N-order bright and dark rogue waves in a resonant erbium-doped fiber system

Jingsong He,[1] Shuwei Xu,[2] and K. Porsezian[3]
[1]*Department of Mathematics, Ningbo University, Ningbo, Zhejiang 315211, P.R. China*
[2]*School of Mathematical Sciences, USTC, Hefei, Anhui 230026, P.R. China*
[3]*Department of Physics, Pondicherry University, Puducherry 605014, India*
(Received 2 October 2012; published 18 December 2012; corrected 6 May 2013)

The rogue waves in a resonant erbium-doped fiber system governed by a coupled system of the nonlinear Schrödinger equation and the Maxwell-Bloch equation (NLS-MB equations) are given explicitly by a Taylor series expansion about the breather solutions of the normalized slowly varying amplitude of the complex field envelope E, polarization p, and population inversion η. The n-order breather solutions of the three fields are constructed using a Darboux transformation (DT) by assuming periodic seed solutions. Moreover, the n-order rogue waves are given by determinant forms with $n+3$ free parameters. Furthermore, the possible connection between our rouge waves and the generation of supercontinuum generation is discussed.

DOI: 10.1103/PhysRevE.86.066603 PACS number(s): 02.30.Ik, 42.81.Dp, 52.35.Bj, 52.35.Sb

I. INTRODUCTION

In recent years, long haul optical communication through fibers has attracted considerable interest in research activities among scientists all over the world. In particular, it has been demonstrated that the soliton-type pulse propagation will play a vital role in the ultrafast communication systems. They are considered to be futuristic tools in achieving low-loss, cost-effective, high-speed communication throughout the world. Soliton-type pulse propagation through nonlinear optical fibers is realized by means of the exact counterbalance between the major constraints of the fiber, *viz.*, group velocity dispersion (linear effect), which broadens the pulse, and the self-phase modulation (nonlinear effect), which contracts the pulse. The propagation of optical pulses through a nonlinear fiber in the picosecond regime is described by the well-known nonlinear Schrödinger (NLS) equation, which was first proposed by Hasegawa and Tappert in 1973 [1].

To make the soliton-based communication systems highly competitive, reliable, and economical when compared to the conventional systems, attenuation in a fiber must be compensated. A different type of optical soliton is associated with the self-induced transparency (SIT) effect in resonant absorbers. The soliton pulse propagation in an erbium-doped fiber amplifier utilizes the SIT phenomenon, first discovered by McCall and Hahn [2]. In 1967 McCall and Hahn proposed a type of optical soliton in a two-level resonant system. Above a well-defined threshold intensity, short resonant pulses of a given duration will propagate through a normally absorbing medium with anomalously low attenuation. This happens when the pulse width is short, compared to the relaxation times in the medium, and the pulse center frequency is in resonance with a two-level absorbing transition. After a few classical absorption lengths, the pulse achieves a steady state in which its width, energy, and shape remain constant. The pulse velocity has greatly reduced from the normal velocity of light in such media. With these properties, the pulse propagation of this type is called a "self-induced transparency" (SIT) soliton and is frequently described by the Maxwell-Bloch (MB) equations:

$$\begin{aligned} E_z &= p, \\ p_t &= i\,\omega_0 p - f q \eta, \\ \eta_t &= f(q p^* + q^* p). \end{aligned} \tag{1}$$

Here E and p are complex variables, η is a real variable, ω_0 is a real constant, and f is the character describing the interaction between the resonant atoms and the optical field. The asterisk symbol denotes the complex conjugate. These equations can be extended to the case of fiber amplifiers. When Er is doped with the core of the optical fibers, then the nonlinear wave propagation can have both effects due to silica and Er impurities. Er impurities give an SIT effect to the optical pulse, whereas the silica material gives the NLS soliton effect. So if we consider these effects for a large width pulse, then the system dynamics will be governed by the coupled system of the NLS equation and the MB equation (NLS-MB system). Considering the erbium doped in nonlinear silica wave guides, for the first time, the combined NLS-MB system was proposed by Maimistov and Manykin [3,4] in 1983. They have also constructed the Lax pair and used the inverse scattering transform technique for the generation of soliton solution. The NLS-MB equations read as [3–5]

$$\begin{aligned} E_t &= i\left[\tfrac{1}{2}E_{xx} + |E|^2 E\right] + 2p, \\ p_x &= 2i\,\omega_0 p + 2E\eta, \\ \eta_x &= -(E p^* + E^* p). \end{aligned} \tag{2}$$

The above equations have also been reduced through Painleve analysis [6]. Further, Kakei and Satsuma [7] also reported the Lax pair and the multisoliton solution of the NLS-MB equations. The integrability aspects of NLS-MB system with variable dispersion, the study of propagation of optical solitons in coupled NLS-MB, and random nonuniform-doped media have been reported earlier wherein the spectral parameter was kept constant. The coexistence of the NLS soliton and SIT soliton has already been confirmed experimentally [10,11]. The propagation and switching of SIT in nonlinear directional couplers with two-level atom nonlinearity has been recently investigated numerically by retaining the transverse dependence of the optical field and atomic variable. Recent experiments by Nakazawa *et al.* have confirmed guided wave SIT soliton formation and propagation by employing a few meters of erbium-doped fiber [8–11].

Recently, considering all higher-order effects in the propagation of femtosecond pulses, the coupled Hirota and Maxwell-Bloch (CH-MB) equations have been proposed and analyzed for soliton solutions [12]. Some generalizations of

NLS-MB equations, for instance, the CH-MB equations and the NLS-MB equations with variable dispersion and nonlinear effects, are discussed [13–15]. The single soliton and the single breather solutions [16] of the NLS-MB equations are given by the Darboux transformation (DT) [17,18]. A soliton solution for the generalized coupled variable coefficient NLS-MB system was also investigated by the DT [19] and the Hirota method [20].

In recent years, in addition to solitons in different optical systems, the study of rogue waves has also attracted considerable interest because of their potential applications in different branches of physics, including oceanography [21–24], which occurs due to either modulation instability [25–31] or a random initial condition [24,32]. The first-order rogue wave is most likely to appear as a single-peak hump with two caves in a plane with a nonzero boundary. One of the possible generating mechanisms for rogue waves is the creation of breathers which can be realized by modulation instability. Then, larger rogue waves can build up when two or more breathers collide into each other [33–39]. Recently more general higher-order rogue waves were obtained, such as showing that these general Nth-order rogue waves contain $(N-1)$ free irreducible complex parameters [37]. Rogue waves can also be observed in space plasmas [40–45] and optics when propagating high-power optical radiation through photonic crystal fibers [46–48]. Considering all higher-order effects in the propagation of femtosecond pulses, rogue waves can also be observed in a system modeled by the Hirota equation [49–51]. Furthermore, rogue waves have not only been observed in continuous media but have also been reported in discrete systems, such as the systems of the well-known Ablowitz-Ladik (A-L) equation [52].

Though the rogue waves have been reported in different branches of physics where the system dynamics is governed by a single equation, to the best of our knowledge, they have been observed and reported seldom in the coupled systems. For example, rogue waves of the coupled NLS were constructed in the literature [53–55]. Very recently, several kinds of matter rogue waves [56] have been reported in the $F=1$ spinor Bose-Einstein condensate system controlled by a three-component NLS equation. In experiment, the rogue waves in a multistable system [57] are revealed by experiments with an erbium-doped fiber laser driven by harmonic pump modulation. So it is our primary interest to analyze the possibility of rogue waves in coupled systems, such as the NLS-MB system.

It is well known that the dark soliton [58] of the defocusing nonlinear Schrödinger (NLS) equation is essentially different from that of the bright soliton. For the past two decades or so, intensive research has been carried by several groups about theoretical and experimental aspects of dark bright solitons. It is quite natural to ask a question: Is there any possibility of observing dark rouge waves in soliton equations? In general, the first-order dark rogue wave has one down dominant peak and two small lumps. Because of the singularity [17,18] of the solution for the defocusing NLS equation generated by using DT, we cannot get defocusing dark rogue waves this way. Fortunately we have obtained dark and bright rogue waves [59] of the NLS-MB equations from a Taylor series expansion of the first-order breather solutions, which are generated from a periodic seed by the DT. But we did not provide a detailed analysis of their dynamical evolution and higher-order rogue waves. The aim of this paper is twofold. First, the determinant representation of the n-fold DT of the NLS-MB equations is similar to the case of the NLS equation DT [60]. Second, the rogue waves of the three optical fields are constructed by determinant forms. It should be noted that the rogue waves of the fields p and η are dark. Furthermore, the connection between our rogue waves and the generation of supercontinuum generation will be discussed.

The organization of this paper is as follows. In Sec. II, the determinant representation of the n-fold DT and formulas of $E^{[n]}$, $p^{[n]}$, and $\eta^{[n]}$ is expressed by eigenfunctions of the spectral problem. In Sec. III, a Taylor series expansion of the breather solutions is generated by n-fold DT from a periodic seed solution with a constant amplitude to construct the bright and dark rogue waves. Moreover, the n-order rogue waves are given by determinant forms with $n+3$ free parameters. Finally, we summarize the results in Sec. IV.

II. DARBOUX TRANSFORMATION

The linear spectral problem of the NLS-MB equations can be expressed as [4]

$$\Psi_x = U\Psi, \tag{3}$$

$$\Psi_t = V\Psi, \tag{4}$$

where

$$\begin{aligned}
\Psi &= \begin{pmatrix} \Psi_1 \\ \Psi_2 \end{pmatrix}, \\
U &= \begin{bmatrix} \lambda & E \\ -E^* & -\lambda \end{bmatrix} \equiv \lambda\sigma_3 + U_0, \\
V &= i\left(\begin{bmatrix} 1 & 0 \\ 0 & -1 \end{bmatrix}\lambda^2 + \begin{bmatrix} 0 & E \\ -E^* & 0 \end{bmatrix}\lambda \right. \\
&\quad \left. + \frac{1}{2}\begin{bmatrix} |E|^2 & E_x \\ E_x^* & -|E|^2 \end{bmatrix}\right) + \frac{1}{\lambda - i\,\omega_0}\begin{pmatrix} \eta & -p \\ -p^* & -\eta \end{pmatrix} \\
&\equiv i\sigma_3\lambda^2 + i\lambda V_1 + \frac{i}{2}V_0 + \frac{1}{\lambda - i\,\omega_0}V_{-1},
\end{aligned}$$

and λ is the complex eigenvalue parameter.

It is easy to prove that the spectral problems (3) and (4) are transformed to

$$\Psi^{[1]}{}_x = U^{[1]}\Psi^{[1]}, \quad U^{[1]} = (T_x + TU)T^{-1}, \tag{5}$$

$$\Psi^{[1]}{}_t = V^{[1]}\Psi^{[1]}, \quad V^{[1]} = (T_t + TV)T^{-1}, \tag{6}$$

under a gauge transformation

$$\Psi^{[1]} = T\Psi. \tag{7}$$

Here T is a 2×2 matrix, which is determined by the cross-differentiating (5) and (6):

$$U^{[1]}{}_t - V^{[1]}{}_x + [U^{[1]}, V^{[1]}] = T(U_t - V_x + [U,V])T^{-1}. \tag{8}$$

This implies that, in order to make Eqs. (3) and (4) invariant under the transformation (7), it is crucial to search a matrix T such that $U^{[1]}$ and $V^{[1]}$ have the same forms as U and V. At the same time the old potential (or seed solutions) (E, p, η) in spectral matrices U and V is mapped into different potentials

(or different solutions) ($E^{[1]}$, $p^{[1]}$, $\eta^{[1]}$) in terms of different spectral matrices $U^{[1]}$ and $V^{[1]}$.

A. One-fold Darboux transformation of NLS-MB equations

In order to be self-contained, we shall recall the one-fold DT [16] of NLS-MB equations. Considering the application of the representation for the n-fold DT by means of the determinant [60] of eigenfunctions with different eigenvalues in the following context, we need to introduce $2n$ eigenfunctions by $f_k = f_k(\lambda_k) = \binom{f_{k1}}{f_{k2}}$ associated with an eigenvalue λ_k, and $\lambda_k = \lambda_m$ if $k = m$, where $k = 1,2,3,\ldots,2n$ but $\lambda_k \neq \lambda$. Additionally, the eigenfunctions for distinct eigenvalues are linearly independent, i.e., f_k and f_m are linearly independent if $k \neq m$.

The elements of one-fold DT [16] are parameterized by the eigenfunction f_k associated with λ_k as

$$T_1(\lambda;\lambda_1,\lambda_2) = \lambda I + S = \begin{pmatrix} \frac{(\widetilde{T_1})_{11}}{|W_2|} & \frac{(\widetilde{T_1})_{12}}{|W_2|} \\ \frac{(\widetilde{T_1})_{21}}{|W_2|} & \frac{(\widetilde{T_1})_{22}}{|W_2|} \end{pmatrix}, \tag{9}$$

where I is a unit matrix, and

$$S = \begin{pmatrix} \frac{\begin{vmatrix} -\lambda_1 f_{11} & f_{12} \\ -\lambda_2 f_{21} & f_{22} \end{vmatrix}}{|W_2|} & \frac{\begin{vmatrix} f_{11} & -\lambda_1 f_{11} \\ f_{21} & -\lambda_2 f_{21} \end{vmatrix}}{|W_2|} \\ \frac{\begin{vmatrix} -\lambda_1 f_{12} & f_{12} \\ -\lambda_2 f_{22} & f_{22} \end{vmatrix}}{|W_2|} & \frac{\begin{vmatrix} f_{11} & -\lambda_1 f_{12} \\ f_{21} & -\lambda_2 f_{22} \end{vmatrix}}{|W_2|} \end{pmatrix},$$

$$W_2(f_1,f_2) = \begin{pmatrix} f_{11} & f_{12} \\ f_{21} & f_{22} \end{pmatrix}, \quad \det(T_1) = (\lambda-\lambda_1)(\lambda-\lambda_2),$$

$$(\widetilde{T_1})_{11} = \begin{vmatrix} 1 & 0 & \lambda \\ f_{11} & f_{12} & \lambda_1 f_{11} \\ f_{21} & f_{22} & \lambda_2 f_{21} \end{vmatrix},$$

$$(\widetilde{T_1})_{12} = \begin{vmatrix} 0 & 1 & 0 \\ f_{11} & f_{12} & \lambda_1 f_{11} \\ f_{21} & f_{22} & \lambda_2 f_{21} \end{vmatrix},$$

$$(\widetilde{T_1})_{21} = \begin{vmatrix} 1 & 0 & 0 \\ f_{11} & f_{12} & \lambda_1 f_{12} \\ f_{21} & f_{22} & \lambda_2 f_{22} \end{vmatrix},$$

$$(\widetilde{T_n})_{22} = \begin{vmatrix} 0 & 1 & \lambda \\ f_{11} & f_{12} & \lambda_1 f_{12} \\ f_{21} & f_{22} & \lambda_2 f_{22} \end{vmatrix}.$$

With the transformed potentials,

$$\begin{aligned} U_0^{[1]} &= U_0 - [\sigma_3, T_1], \\ V_{-1}^{[1]} &= T_1\big|_{\lambda=i\omega_0} V_{-1} {T_1}^{-1}\big|_{\lambda=i\omega_0}, \end{aligned} \tag{10}$$

the resulting solutions of $E^{[1]}$, $p^{[1]}$, and $\eta^{[1]}$ are given by

$$E^{[1]} = E - 2S_{12}, \tag{11}$$

$$\begin{aligned} p^{[1]} = -\frac{1}{\det(T_1)}[&-2\eta(T_1)_{11}(T_1)_{12} + p^*(T_1)_{12}(T_1)_{12} \\ &- p(T_1)_{11}(T_1)_{11}]|_{\lambda=i\omega_0}, \end{aligned} \tag{12}$$

$$\begin{aligned} \eta^{[1]} = \frac{1}{\det(T_1)}[&\eta((T_1)_{11}(T_1)_{22} + (T_1)_{12}(T_1)_{21}) \\ &- p^*(T_1)_{12}(T_1)_{22} + p(T_1)_{11}(T_1)_{21}]|_{\lambda=i\omega_0}, \end{aligned} \tag{13}$$

and the resulting eigenfunction $f_k^{[1]}$ of λ_k corresponding to the resulting potentials is

$$f_k^{[1]} = \begin{pmatrix} \frac{\begin{vmatrix} f_{k1} & f_{k2} & \lambda_k f_{k1} \\ f_{11} & f_{12} & \lambda_1 f_{11} \\ f_{21} & f_{22} & \lambda_2 f_{21} \end{vmatrix}}{|W_2|} \\ \frac{\begin{vmatrix} f_{k1} & f_{k2} & \lambda_k f_{k2} \\ f_{11} & f_{12} & \lambda_1 f_{12} \\ f_{21} & f_{22} & \lambda_2 f_{22} \end{vmatrix}}{|W_2|} \end{pmatrix}.$$

In order to satisfy the constraints of S' and V'_{-1} in Ref. [16], set

$$\lambda_2 = -\lambda_1^*, f_2 = \begin{pmatrix} -f_{12}^* \\ f_{11}^* \end{pmatrix}. \tag{14}$$

B. n-fold Darboux transformation for NLS-MB equations

In this subsection, our primary aim is to establish the determinant representation of the n-fold DT for NLS-MB equations as we have done for the case of the NLS equation [60]. According to the form of T_1 in Eq. (9), the n-fold DT should be of the form $T_n = T_n(\lambda) = \lambda^n I + t_1\lambda^{n-1} + t_2\lambda^{n-2} + \cdots + t_{n-1}\lambda + t_n$, where t_i are 2×2 matrices, $i = 1,2,\ldots,n$, and T_n leads to the determinant representation of T_n by means of its kernel. Specifically, from algebraic equations,

$$\begin{aligned} f_k^{[n]} &= T_n(\lambda;\lambda_1,\lambda_2,\ldots,\lambda_{2n-1},\lambda_{2n})|_{\lambda=\lambda_i} f_k \\ &= \sum_{l=0}^{n} t_l \lambda_k^l f_k = 0, i = 1,2,\ldots,2n-1,2n, \end{aligned} \tag{15}$$

with

$$t_0 = \begin{pmatrix} 1 & 0 \\ 0 & 1 \end{pmatrix},$$

coefficients $t_l, l = 1,2,\ldots,n$ are solved by Cramer's rule. Thus we obtain the determinant representation of the T_n.

Theorem 1. The n-fold DT of the NLS-MB equations is $T_n = T_n(\lambda) = \lambda^n I + t_1\lambda^{n-1} + t_2\lambda^{n-2} + \cdots + t_{n-1}\lambda + t_n$, where t_i are 2×2 matrices, $i = 1,2,\ldots,n$. The final form of $T_n(\lambda)$ has the form

$$T_n = T_n(\lambda;\lambda_1,\lambda_2,\ldots,\lambda_{2n-1},\lambda_{2n}) = \begin{pmatrix} \frac{(\widetilde{T_n})_{11}}{|W_{2n}|} & \frac{(\widetilde{T_n})_{12}}{|W_{2n}|} \\ \frac{(\widetilde{T_n})_{21}}{|W_{2n}|} & \frac{(\widetilde{T_n})_{22}}{|W_{2n}|} \end{pmatrix}, \tag{16}$$

where I is a unit matrix, and expressions for t_1 and components of T_n are given in Appendix A.

It is easy to construct a simple form of the determinant of T_n:

$$\det(T_n) = (\lambda-\lambda_1)(\lambda-\lambda_2)\cdots(\lambda-\lambda_{2n-1})(\lambda-\lambda_{2n}).$$

Next, we consider the transformed resulting solutions $(E^{[n]}, p^{[n]}, \eta^{[n]})$ of NLS-MB equations corresponding to the n-fold DT.

Corollary 1. For the n-fold DT, the transformed potentials are

$$\begin{aligned} U_0^{[n]} &= U_0 - [\sigma_3, T_n], \\ V_{-1}^{[n]} &= T_n\big|_{\lambda=i\omega_0} V_{-1} {T_n}^{-1}\big|_{\lambda=i\omega_0}, \end{aligned} \tag{17}$$

which leads to the resulting solutions $E^{[n]}$, $p^{[n]}$, and $\eta^{[n]}$ of the form

$$E^{[n]} = E - 2(t_1)_{12}, \tag{18}$$

$$p^{[n]} = -\frac{1}{\det(T_n)}[-2\eta(T_n)_{11}(T_n)_{12} + p^*(T_n)_{12}(T_n)_{12} - p(T_n)_{11}(T_n)_{11}]|_{\lambda=i\omega_0}, \tag{19}$$

$$\eta^{[n]} = \frac{1}{\det(T_n)}\{\eta[(T_n)_{11}(T_n)_{22} + (T_n)_{12}(T_n)_{21}] - p^*(T_n)_{12}(T_n)_{22} + p(T_n)_{11}(T_n)_{21}\}|_{\lambda=i\omega_0}, \tag{20}$$

and the resulting eigenfunction $f_k^{[n]}$ of λ_k is

$$f_k^{[n]} = \left(\frac{\begin{vmatrix} f_{k1} & f_{k2} & \lambda_k f_{k1} & \lambda_k f_{k2} & \lambda_k^2 f_{k1} & \lambda_k^2 f_{k2} & \dots & \lambda_k^{n-1} f_{k1} & \lambda_k^{n-1} f_{k2} & \lambda_k^n f_{k1} \\ f_{11} & f_{12} & \lambda_1 f_{11} & \lambda_1 f_{12} & \lambda_1^2 f_{11} & \lambda_1^2 f_{12} & \dots & \lambda_1^{n-1} f_{11} & \lambda_1^{n-1} f_{12} & \lambda_1^n f_{11} \\ f_{21} & f_{22} & \lambda_2 f_{21} & \lambda_2 f_{22} & \lambda_2^2 f_{21} & \lambda_2^2 f_{22} & \dots & \lambda_2^{n-1} f_{21} & \lambda_2^{n-1} f_{22} & \lambda_2^n f_{21} \\ f_{31} & f_{32} & \lambda_3 f_{31} & \lambda_3 f_{32} & \lambda_3^2 f_{31} & \lambda_3^2 f_{32} & \dots & \lambda_3^{n-1} f_{31} & \lambda_3^{n-1} f_{32} & \lambda_3^n f_{31} \\ \vdots & \vdots & \vdots & \vdots & \vdots & \vdots & \vdots & \vdots & \vdots & \vdots \\ f_{2n1} & f_{2n2} & \lambda_{2n} f_{2n1} & \lambda_{2n} f_{2n2} & \lambda_{2n}^2 f_{2n1} & \lambda_{2n}^2 f_{2n2} & \dots & \lambda_{2n}^{n-1} f_{2n1} & \lambda_{2n}^{n-1} f_{2n2} & \lambda_{2n}^n f_{2n1} \end{vmatrix}}{|W_{2n}|} \right.$$

$$\left. \frac{\begin{vmatrix} f_{k1} & f_{k2} & \lambda_k f_{k1} & \lambda_k f_{k2} & \lambda_k^2 f_{k1} & \lambda_k^2 f_{k2} & \dots & \lambda_k^{n-1} f_{k1} & \lambda_k^{n-1} f_{k2} & \lambda_k^n f_{k2} \\ f_{11} & f_{12} & \lambda_1 f_{11} & \lambda_1 f_{12} & \lambda_1^2 f_{11} & \lambda_1^2 f_{12} & \dots & \lambda_1^{n-1} f_{11} & \lambda_1^{n-1} f_{12} & \lambda_1^n f_{12} \\ f_{21} & f_{22} & \lambda_2 f_{21} & \lambda_2 f_{22} & \lambda_2^2 f_{21} & \lambda_2^2 f_{22} & \dots & \lambda_2^{n-1} f_{21} & \lambda_2^{n-1} f_{22} & \lambda_2^n f_{22} \\ f_{31} & f_{32} & \lambda_3 f_{31} & \lambda_3 f_{32} & \lambda_3^2 f_{31} & \lambda_3^2 f_{32} & \dots & \lambda_3^{n-1} f_{31} & \lambda_3^{n-1} f_{32} & \lambda_3^n f_{32} \\ \vdots & \vdots & \vdots & \vdots & \vdots & \vdots & \vdots & \vdots & \vdots & \vdots \\ f_{2n1} & f_{2n2} & \lambda_{2n} f_{2n1} & \lambda_{2n} f_{2n2} & \lambda_{2n}^2 f_{2n1} & \lambda_{2n}^2 f_{2n2} & \dots & \lambda_{2n}^{n-1} f_{2n1} & \lambda_{2n}^{n-1} f_{2n2} & \lambda_{2n}^n f_{2n2} \end{vmatrix}}{|W_{2n}|} \right). \tag{21}$$

Note that

$$\lambda_{2k} = -\lambda_{2k-1}^*, \quad f_{2k} = \begin{pmatrix} -f_{2k-12}^* \\ f_{2k-11}^* \end{pmatrix}$$

in order to satisfy the constraints of DT.

III. *N*-ORDER BRIGHT AND DARK ROGUE WAVES GENERATED BY *N*-ORDER BREATHER SOLUTIONS

By using the results of DT discussed above, breather solutions of E, p, and η of NLS-MB equations are generated by assuming a periodic seed solution. Then we can construct the explicit bright and dark rogue waves of the NLS-MB equations through a Taylor series expansion of the breather solutions.

Substituting $E = d\exp[i\rho]$, $p = ifE$, $\eta = 1$ into the spectral problem Eqs. (3) and (4), and using the method of separation of variables and the superposition principle, the eigenfunction f_{2k-1} associated with λ_{2k-1} is given by

$$\begin{pmatrix} f_{2k-11}(x,t,\lambda_{2k-1}) \\ f_{2k-12}(x,t,\lambda_{2k-1}) \end{pmatrix} = \begin{pmatrix} C_1\varpi(x,t,\lambda_{2k-1})[1,2k-1] - C_2\varpi^*(x,t,-\lambda_{2k-1}^*)[2,2k-1] \\ C_1\varpi(x,t,\lambda_{2k-1})[2,2k-1] + C_2\varpi^*(x,t,-\lambda_{2k-1}^*)[1,2k-1] \end{pmatrix}, \tag{22}$$

where

$$\begin{pmatrix} \varpi(x,t,\lambda_{2k-1})[1,2k-1] \\ \varpi(x,t,\lambda_{2k-1})[2,2k-1] \end{pmatrix} = \begin{pmatrix} d\exp\left[\frac{i}{2}\rho + ic(\lambda_{2k-1})\right] \\ \left[i\left(c_1(\lambda_{2k-1}) + \frac{b}{2}\right) - \lambda_{2k-1}\right]\exp\left[-\frac{i}{2}\rho + ic(\lambda_{2k-1})\right] \end{pmatrix},$$

$$\varpi(x,t,\lambda_{2k-1}) = \begin{pmatrix} \varpi(x,t,\lambda_{2k-1})[1,2k-1] \\ \varpi(x,t,\lambda_{2k-1})[2,2k-1] \end{pmatrix}.$$

Note that $\varpi(x,t,\lambda_{2k-1})$ is the basic solution of the spectral problem [Eqs. (3) and (4)]. Here $a, b, d, t, z \in \mathbb{R}$, $C_1, C_2 \in \mathbb{C}$:

$$c(\lambda_{2k-1}) = c_1(\lambda_{2k-1})x + c_2(\lambda_{2k-1})t,$$

$$c_1(\lambda_{2k-1}) = \sqrt{d^2 - \left(\frac{ib}{2} - \lambda_{2k-1}\right)^2},$$

$$c_2(\lambda_{2k-1}) = \left(i\lambda_{2k-1} - \frac{b}{2} - \frac{if}{\lambda_{2k-1} - i\omega_0}\right)c_1(\lambda_{2k-1}),$$

$$\rho = a\,t + b\,x,$$

$$f = \frac{1}{2}\left(a + \frac{b^2}{2} - d^2\right),$$

and $(-b + 2\omega_0)f = 2$ is used for f.

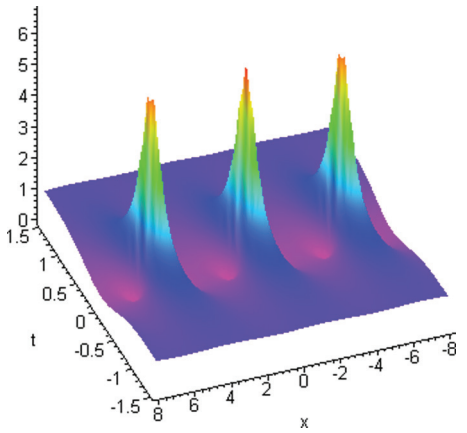

FIG. 1. (Color online) The first-order breather $|E^{[1]}|^2$ given with specific parameters $d = 1$, $b = 2$, $\omega_0 = \frac{1}{2}$, $\alpha_1 = \frac{4}{5}$. There are one upper peak and two caves in each periodic unit.

A. The *n*-order breather solutions of NLS-MB equations

For simplicity, under the condition $C_1 = C_2 = 1$, let $\lambda_{2k-1} = \alpha_{2k-1} + i\frac{b}{2}$, such that $\mathrm{Im}(\frac{ib}{2} - \lambda_{2k-1}) = 0$ and $c_1(\lambda_{2k-1}) = \sqrt{d^2 - \mathrm{Re}^2(\lambda_{2k-1})} \in \mathbb{R}$, and using Eq. (21), then substituting eigenfunctions Eq. (22) into Eq. (16), we obtain the determinant representation of DT in the form which is discussed in Appendix B.

Using Eq. (A1) in Eqs. (18)–(20) with the choice of Eq. (A2), we can construct $E^{[n]}$, $p^{[n]}$, and $\eta^{[n]}$. For brevity, in the following, we are giving only an explicit expression of $E^{[1]}$ with specific parameters $d = 1$, $b = 2$, $\omega_0 = \frac{1}{2}$:

$$
\begin{aligned}
E^{[1]} &= E + 4\alpha_1 \frac{v_3}{v_4} \exp[i(-5t + 2x)],\\
v_3 &= -\alpha_1 \cos(2w_1) + \big[2\cos(w_1) + 2\sqrt{1-\alpha_1^2}\sin(w_1)\alpha_1\\
&\quad + 2\alpha_1^2\cos(w_1)\big]\cosh(w_2) + \big[2i\alpha_1^2\sin(w_1)\\
&\quad - 2i\sin(w_1) - 2i\alpha_1\cos(w_1)\sqrt{1-\alpha_1^2}\big]\sinh(w_2)\\
&\quad - 2\alpha_1 - \sqrt{1-\alpha_1^2}\sin(2w_1)\\
&\quad + i\sqrt{1-\alpha_1^2}\sinh(2w_2) - \alpha_1\cosh(2w_2),\\
v_4 &= 2\alpha_1^2\cos(2w_1) - 2\big[4\alpha_1\cos(w_1)\\
&\quad + 2\sin(w_1)\sqrt{1-\alpha_1^2}\big]\cosh(w_2)\\
&\quad - 2\big[-1-\alpha_1^2 - \cosh(2w_2) - \sqrt{1-\alpha_1^2}\alpha_1\sin(2w_1)\big],\\
w_1 &= -2\sqrt{1-\alpha_1^2}x + \frac{12}{5}\sqrt{1-\alpha_1^2}t,\\
w_2 &= \frac{26}{5}\sqrt{1-\alpha_1^2}t.
\end{aligned}
$$

The dynamical evolution of $|E^{[1]}|^2$, $|p^{[1]}|^2$, and $\eta^{[1]}$ for the parametric choice $d = 1$, $b = 2$, $\omega_0 = \frac{1}{2}$, $\alpha_1 = 0.8$ is plotted in Figs. 1–3, which confirms the direct verification of the periodic as well as decaying properties of typical breather solutions. The breather of $E^{[1]}$ is almost same as that of the NLS equation, which has one upper peak and two caves in each periodic unit. On the other hand, we observe that the resulting

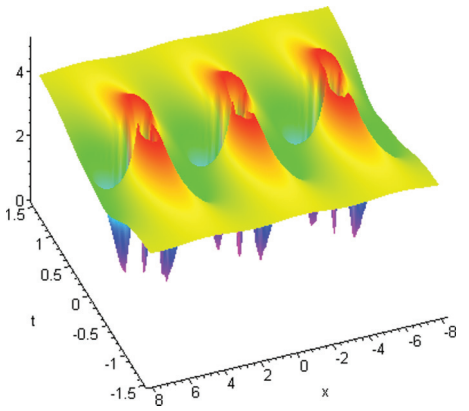

FIG. 2. (Color online) The first-order dark breather $|p^{[1]}|^2$ for the values used in Fig. 1. There are a upper ring and three down peaks in each periodic unit.

kinds of breathers for $p^{[1]}$ and $\eta^{[1]}$ are also different. It is interesting to note that the resulting breather $p^{[1]}$ admits one upper ring and three down peaks in each periodic unit, whereas the resulting breather $\eta^{[1]}$ has two lumps and one down peak in each periodic unit. Moreover, these two breathers can be called dark breathers because the down amplitude is dominant in both the cases. The above discussed properties are clearly seen in Figs. 1–3.

B. The first-order rogue waves generated by first-order breather solutions

Similarly, under the condition $C_1 = C_2 = 1$, substituting eigenfunctions Eq. (22) into Eqs. (18)–(20) with $\lambda_1 = \alpha_1 + i\frac{b}{2}$, by assuming $\alpha_1 \to d (d > 0)$, $E^{[1]}$, $p^{[1]}$, and $\eta^{[1]}$ become rational solutions $\{\tilde{E}^{[1]}, \tilde{p}^{[1]}, \tilde{\eta}^{[1]}\}$ in the form of rogue waves [59]. When $x \to \infty$, $t \to \infty$ in the above expressions, after some manipulations, we find

$$
|\tilde{E}^{[1]}|^2 \to d^2, \quad |\tilde{p}^{[1]}|^2 \to \frac{d^2}{\left(\frac{b}{2} - \omega_0\right)^2}, \quad \text{and} \quad \tilde{\eta}^{[1]} \to 1.
$$

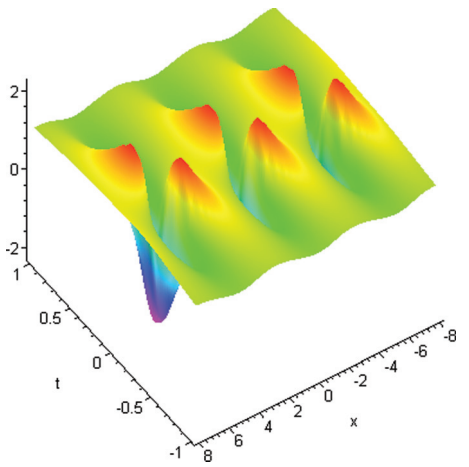

FIG. 3. (Color online) The first-order dark breather $\eta^{[1]}$ for the values used in Fig. 1. There are two lumps and one down peak in each periodic unit.

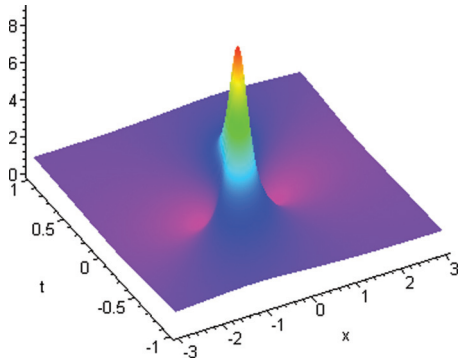

FIG. 4. (Color online) The first-order rogue wave $|\tilde{E}^{[1]}|^2$ with specific parameters $d = 1$, $b = 2$, $\omega_0 = \frac{1}{2}$. There are one upper peak and two caves.

In addition to the above conditions, from $|\tilde{E}^{[1]}|^2_x = 0$ and $|\tilde{E}^{[1]}|^2_t = 0$, we also observe that the maximum amplitude of $|\tilde{E}^{[1]}|^2$ occurs at $t = 0$ and $x = 0$ and is equal to $9d^2$, and the minimum amplitude of $|\tilde{E}^{[1]}|^2$ occurs at $t = 0$ and $x = \pm\frac{\sqrt{3}}{2d}$ and is equal to 0. By using a similar procedure discussed above, we can also obtain the extreme value of $|\tilde{p}^{[1]}|^2$ and $\tilde{\eta}^{[1]}$.

Figure 4 is plotted for the rogue wave $|\tilde{E}^{[1]}|^2$ with specific parameters $d = 1$, $b = 2$, $\omega_0 = \frac{1}{2}$. From Fig. 4, we infer the following interesting results: (1) $|\tilde{E}^{[1]}|^2 \to 1$ by assuming $x \to \infty$, $t \to \infty$, which gives the asymptotic plane; (2) the maximum amplitude of $|\tilde{E}^{[1]}|^2$ occurs at $t = 0$ and $x = 0$ and is equal to 9, and the minimum amplitude of $|\tilde{E}^{[1]}|^2$ occurs at $t = 0$ and $x = \pm\frac{\sqrt{3}}{2}$ and is equal to 0. As the general expression of the extreme values of $|p^{[1]}|^2$ and $\tilde{\eta}^{[1]}$ is quite complicated in nature, for simplicity, we discuss only these solutions under a certain choice of parameters.

Figure 5 is plotted for the rogue wave $|\tilde{p}^{[1]}|^2$ on a $(x\text{-}t)$ plane with the above parameters. Like in the earlier case, here as well we observe the following salient features: (1) the height of the asymptotical plane is 4 because $|\tilde{p}^{[1]}|^2 \to 4$, when $x \to \infty$, $t \to \infty$; (2) the maximum amplitude of $|\tilde{p}^{[1]}|^2$ occurs in the form of a ring curve on a $(x\text{-}t)$ plane defined by

$$-\frac{507}{16}t^2 + \frac{1681}{8}t^4 + \frac{25}{8}x^4 - \frac{55}{128} + \frac{65}{16}x^2 + \frac{277}{4}x^2t^2 - 15x^3t + \frac{65}{4}xt - 123xt^3 = 0$$

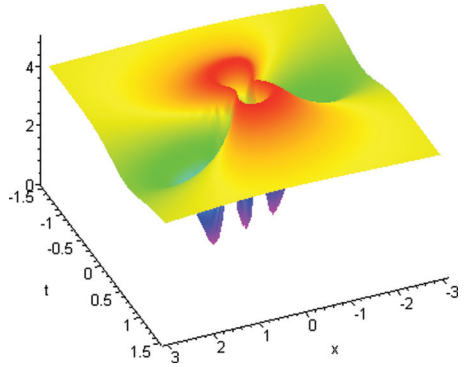

FIG. 5. (Color online) The first-order dark rogue wave $|\tilde{p}^{[1]}|^2$ for the values used in Fig. 4. There are one upper ring and three down peaks.

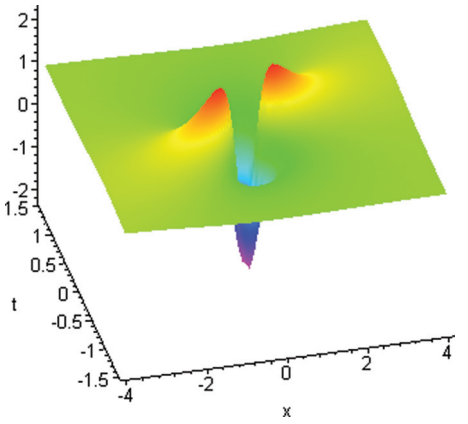

FIG. 6. (Color online) The first-order dark rogue wave $\tilde{\eta}^{[1]}$ for the values used in Fig. 4. There are two lumps and one down peak.

and is equal to 5, and the minimum amplitude of $|\tilde{p}^{[1]}|^2$ occurs at four points:

$$\left\{\left(t = \frac{+5+\sqrt{5}}{52}, \quad x = \frac{+19+9\sqrt{5}}{52}\right), \left(t = \frac{+5-\sqrt{5}}{52}, \quad x = \frac{+19-9\sqrt{5}}{52}\right), \left(t = \frac{-5+\sqrt{5}}{52}, \quad x = \frac{-19+9\sqrt{5}}{52}\right), \left(t = \frac{-5-\sqrt{5}}{52}, \quad x = \frac{-19-9\sqrt{5}}{52}\right)\right\}$$

and is equal to 0; 3) the extreme value of the amplitude $|\tilde{p}^{[1]}|^2$ occurs at $t = 0$ and $x = 0$ and is equal to $\frac{4}{25}$. We also observe that the middle down peak in Fig. 5 has two subpeaks. Due to the direction of the observation of the figure, these two close subpeaks are not clearly distinguished from the figure; we just find three down peaks.

Figure 6 is plotted for the rogue wave $\tilde{\eta}^{[1]}$ with specific parameters as in Fig. 4. From the figure, we observe the following results: 1) the height of the asymptotical plane is 1 because $\tilde{\eta}^{[1]} \to 1$ by letting $x \to \infty$, $t \to \infty$; 2) the maximum

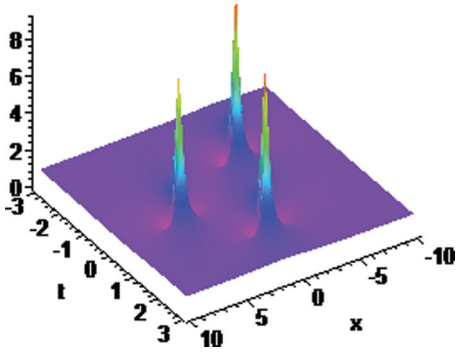

FIG. 7. (Color online) The second-order rogue wave $|\tilde{E}^{[2]}|^2$ given by Eq. (25) with specific parameters $d = 1$, $b = 2$, $\omega_0 = \frac{1}{2}$, $K_0 = 1$, $J_0 = 0$, $J_1 = 100$.

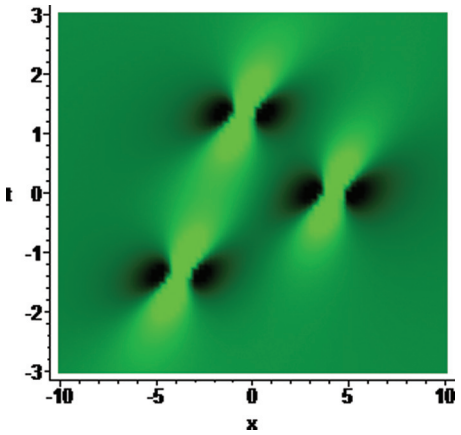

FIG. 8. (Color online) Contour plot of the wave amplitudes of $|\bar{E}^{[2]}|^2$ for the values used in Fig. 7.

amplitude of $\tilde{\eta}^{[1]}$ occurs at two points:

$$\left\{\left(t=+\frac{5+\sqrt{5}}{52},\quad x=+\frac{19+9\sqrt{5}}{52}\right)\right\}$$

and

$$\left\{\left(t=-\frac{5+\sqrt{5}}{52},\quad x=-\frac{19+9\sqrt{5}}{52}\right)\right\}$$

and is equal to $\sqrt{5}$, and the minimum amplitude of $\tilde{\eta}^{[1]}$ occurs at two points:

$$\left\{\left(t=\frac{+5-\sqrt{5}}{52},\quad x=\frac{+19-9\sqrt{5}}{52}\right)\right\}$$

and

$$\left\{\left(t=\frac{-5+\sqrt{5}}{52},\quad x=\frac{-19+9\sqrt{5}}{52}\right)\right\}$$

and is equal to $-\sqrt{5}$; (3) the extreme value of the amplitude $\tilde{\eta}^{[1]}$ occurs at $t=0$ and $x=0$ and is equal to $-\frac{11}{5}$. Like in Fig. 5, here also we observe that the down peak in Fig. 6 has two subpeaks.

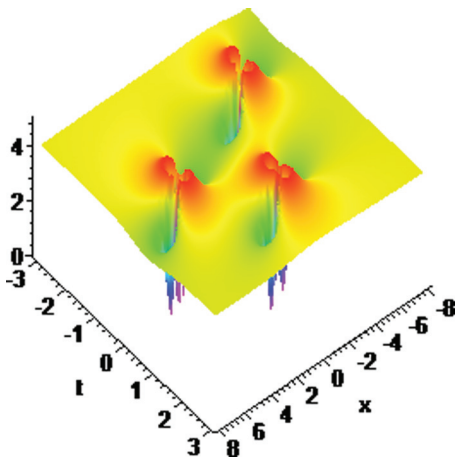

FIG. 9. (Color online) The second-order dark rogue wave $|\tilde{p}^{[2]}|^2$ given by Eq. (26) for the values used in Fig. 7.

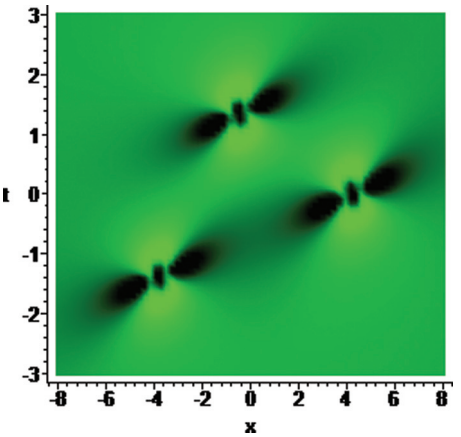

FIG. 10. (Color online) Contour plot of the wave amplitudes of $|\bar{p}^{[2]}|^2$ for the values used in Fig. 7.

C. The higher-order rogue waves and their determinant forms

In order to emphasize the richness of the higher-order rogue waves, we can modify C_1 and C_2 in Eq. (22) as the following:

$$C_1=K_0+\exp\left\{ic_1(\lambda_{2k-1})\sum_{j=0}^{k-1}J_j\left[\lambda_{2k-1}-\left(d+i\frac{b}{2}\right)\right]^j\right\},$$
$$C_2=K_0+\exp\left\{-ic_1(\lambda_{2k-1})\sum_{j=0}^{k-1}J_j\left[\lambda_{2k-1}-\left(d+i\frac{b}{2}\right)\right]^j\right\}, \tag{23}$$

where $K_0,\ J_j\in\mathbb{C}$. Note that $\lambda_{2k-1}=d+i\frac{b}{2}$ is the zero point of $c_1(\lambda_{2k-1})$.

Based on Sec. III B, higher-order rogue waves can be constructed by the breather solutions. In other words, let $\lambda_{2k-1}\to d+i\frac{b}{2}$ in n-order breather solutions; n-order rogue waves can be given. Generally, in comparison to the method of

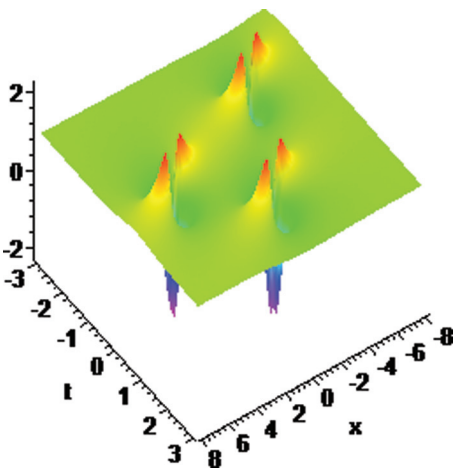

FIG. 11. (Color online) The second-order dark rogue wave $\bar{\eta}^{[2]}$ given by Eq. (27) for the values used in Fig. 7.

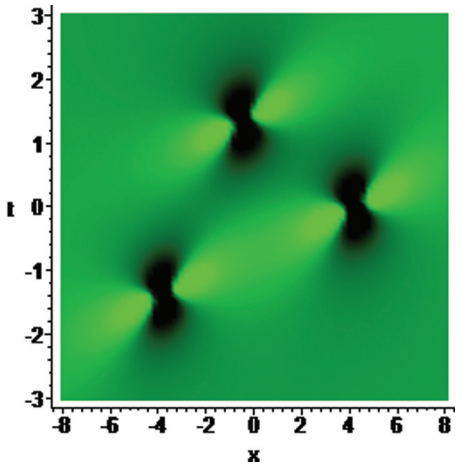

FIG. 12. (Color online) Contour plot of the wave amplitudes of $\bar{\eta}^{[2]}$ for the values used in Fig. 7.

limiting the breather solutions, the method of making a rational eigenfunction below may be more direct, and the rogue wave can be shown by determinant forms.

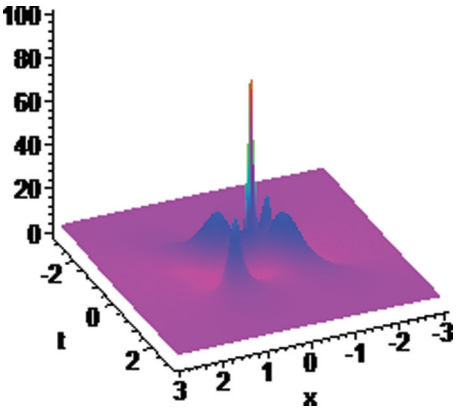

FIG. 13. (Color online) The second-order rogue wave $|\bar{E}^{[2]}|^2$ given by Eq. (25) with specific parameters $d = 2, b = 0, \omega_0 = \frac{1}{2}$, $K_0 = 1$, $J_0 = 0$, $J_1 = 0$.

Substituting Eq. (23) into Eq. (22), by assuming $\lambda_{2k-1} \to d + i\frac{b}{2}$, eigenfunction f_{2k-1} associated with λ_{2k-1} becomes a rational eigenfunction f_r as follows:

$$\begin{pmatrix} f_{r1} \\ f_{r2} \end{pmatrix} = \begin{pmatrix} -\left\{(2dK_0 + 2d)x + 2\left[\frac{2i}{(b-2\omega_0)\left(d+\frac{1}{2}ib-i\omega_0\right)} + id - b\right](K_0+1)dt + 2J_0 d + K_0 + 1\right\}\sqrt{2d}\exp(K) \\ -\left\{-(2dK_0 + 2d)x - 2\left[\frac{2i}{(b-2\omega_0)\left(d+\frac{1}{2}ib-i\omega_0\right)} + id - b\right](K_0+1)dt - 2J_0 d + K_0 + 1\right\}\sqrt{2d}\exp(-K) \end{pmatrix},$$

$$K = \frac{1}{2}i\left[-\frac{8 + b^3 - 2b^2\omega_0 - 2d^2 b + 4d^2\omega_0}{2(b-2\omega_0)}t + bx\right]. \tag{24}$$

Substituting eigenfunctions Eq. (24) into Eqs. (11)–(13), we can get the first-order rogue waves $\{\bar{E}^{[1]}, \bar{p}^{[1]}, \bar{\eta}^{[1]}\}$ in the form of determinant. The dynamical evolution of $|\bar{E}^{[1]}|^2$, $|\bar{p}^{[1]}|^2$, and $\bar{\eta}^{[1]}$ for the parametric choice d, b, ω_0, K_0, J_0 is respectively similar to Figs. 4–6, but we can control the position of the first-order rogue waves by choosing the parameters K_0 and J_0.

Theorem 2. For the n-fold DT, the n-order rogue waves $\bar{E}^{[n]}$, $\bar{p}^{[n]}$, and $\bar{\eta}^{[n]}$ are of the form

$$\bar{E}^{[n]} = E - 2(\bar{t}_{r1})_{12}, \tag{25}$$

$$\bar{p}^{[n]} = -\frac{1}{\det(\bar{T}_{rn})}[-2\eta(\bar{T}_{rn})_{11}(\bar{T}_{rn})_{12} + p^*(\bar{T}_{rn})_{12}(\bar{T}_{rn})_{12} - p(\bar{T}_{rn})_{11}(\bar{T}_{rn})_{11}]|_{\lambda=i\omega_0}, \tag{26}$$

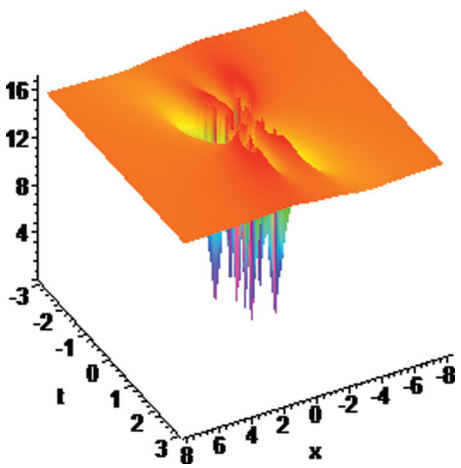

FIG. 14. (Color online) The second-order dark rogue wave $|\bar{p}^{[2]}|^2$ given by Eq. (26) for the values used in Fig. 13.

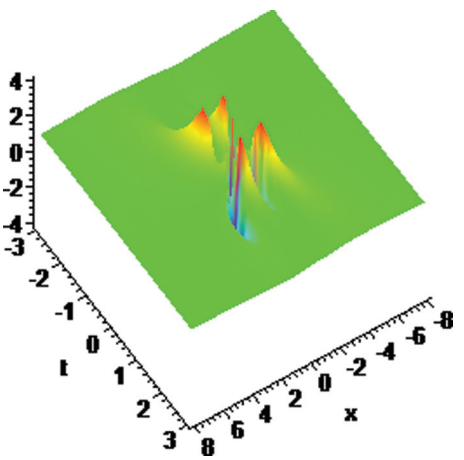

FIG. 15. (Color online) The second-order dark rogue wave $\bar{\eta}^{[2]}$ given by Eq. (27) for the values used in Fig. 13.

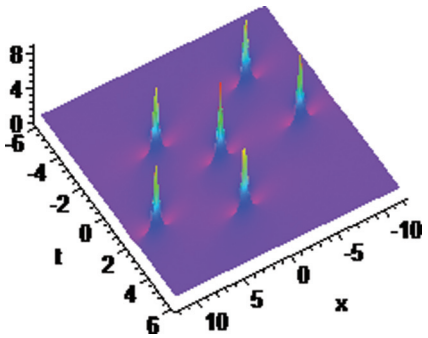

FIG. 16. (Color online) The third-order rogue wave $|\bar{E}^{[3]}|^2$ given by Eq. (25) with specific parameters $d = 1$, $b = 2$, $\omega_0 = \frac{1}{2}$, $K_0 = 1$, $J_0 = 0$, $J_1 = 0$, $J_2 = 8000$.

$$\bar{\eta}^{[n]} = \frac{1}{\det(\bar{T}_{rn})}[\eta((\bar{T}_{rn})_{11}(\bar{T}_{rn})_{22} + (\bar{T}_{rn})_{12}(\bar{T}_{rn})_{21}) - p^*(\bar{T}_{rn})_{12}(\bar{T}_{rn})_{22} + p(\bar{T}_{rn})_{11}(\bar{T}_{rn})_{21}]|_{\lambda=i\omega_0}. \quad (27)$$

The final form of $\bar{T}_{rn}(\lambda)$ is given in Appendix C.

Case 1. When $n = 2$, substituting Eq. (B1) into Eqs. (25)–(27) can give the second-order rogue waves with five free parameters. Note that under the condition $J_1 \gg J_0$, the second-order rogue wave can split into three first-order rogue wave (triplets rogue wave) [61] rather than two. The dynamical evolution of $|\bar{E}^{[2]}|^2$, $|\bar{p}^{[2]}|^2$, and $\bar{\eta}^{[2]}$ for the parametric choice $d = 1$, $b = 2$, $\omega_0 = \frac{1}{2}$, $K_0 = 1$, $J_0 = 0$, $J_1 = 100$ is plotted in Figs. 7, 9, and 11 and their corresponding density plots are shown in Figs. 8, 10, and 12. There is another kind of second-order rogue wave; for example, $|\bar{E}^{[2]}|^2$ is higher than the second-order rogue wave above. The dynamical evolution of $|\bar{E}^{[2]}|^2$, $|\bar{p}^{[2]}|^2$, and $\bar{\eta}^{[2]}$ for the parametric choice $d = 2$, $b = 0$, $\omega_0 = \frac{1}{2}$, $K_0 = 1$, $J_0 = 0$, $J_1 = 0$ is plotted in Figs. 13–15. Note that eigenvalue $\lambda_1 = \lambda_3$ is real. The eigenvalue of rogue waves is different from the eigenvalue of solutions given in the past.

Case 2. When $n = 3$, substituting Eq. (B1) into Eqs. (25)–(27) can give the third-order rogue waves with six free parameters. Note that under the condition $J_2 \gg J_i$ $(i = 0,1)$ or $J_1 \gg J_i (i = 0,2)$, the third-order rogue wave can split into six first-order rogue waves instead. Circular rogue wave [62] may be constructed by the condition $J_2 \gg J_1$ and $J_2 \gg J_0$. The dynamical evolution of $|\bar{E}^{[3]}|^2$, $|\bar{p}^{[3]}|^2$, and $\bar{\eta}^{[3]}$ for the parametric choice $d = 1$, $b = 2$, $\omega_0 = \frac{1}{2}$, $K_0 = 1$, $J_0 = 0$, $J_1 = 0$, $J_2 = 8000$ is plotted in Figs. 16–18. At the same time, rogue wave triplets may be constructed by the condition $J_1 \gg J_2$ and $J_1 \gg J_0$. The dynamical evolution of $|\bar{E}^{[3]}|^2$, $|\bar{p}^{[3]}|^2$, and $\bar{\eta}^{[3]}$ for the parametric choice $d = 1$, $b = 2$, $\omega_0 = \frac{1}{2}$, $K_0 = 1$, $J_0 = 0$, $J_1 = 100$, $J_2 = 0$ is plotted in Figs. 19–21. Similarly, there is another kind third-order rogue wave; for example, $|\bar{E}^{[3]}|^2$ is higher than third-rogue above. The dynamical evolution of $|\bar{E}^{[3]}|^2$, $|\bar{p}^{[3]}|^2$, and $\bar{\eta}^{[3]}$ for the parametric choice $d = \frac{4}{3}$, $b = 0$, $\omega_0 = \frac{1}{2}$, $K_0 = 1$, $J_0 = 0$, $J_1 = 0$, $J_2 = 0$ is plotted in Figs. 22–24. Note that eigenvalue $\lambda_1 = \lambda_3 = \lambda_5$ is real. The eigenvalue of rogue waves is different from the eigenvalue of solutions given in the past. According to analysis above, the n-order rogue waves may be controlled by $n + 3$ free parameters.

From the above discussions, it is interesting to point out that the down amplitudes are dominant in the profile of rogue

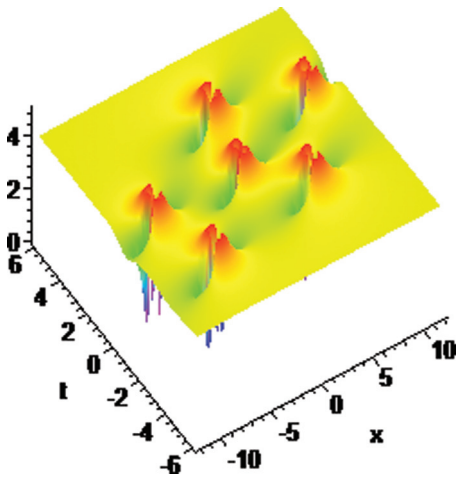

FIG. 17. (Color online) The third-order dark rogue wave $|\bar{p}^{[3]}|^2$ given by Eq. (26) for the values used in Fig. 16.

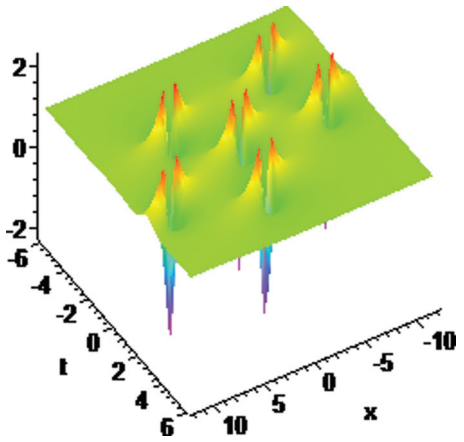

FIG. 18. (Color online) The third-order dark rogue wave $\bar{\eta}^{[3]}$ given by Eq. (27) for the values used in Fig. 16.

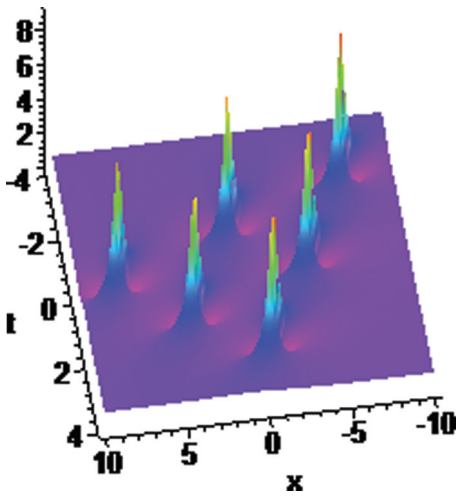

FIG. 19. (Color online) The third-order rogue wave $|\bar{E}^{[3]}|^2$ given by Eq. (25) with specific parameters $d = 1$, $b = 2$, $\omega_0 = \frac{1}{2}$, $K_0 = 1$, $J_0 = 0$, $J_1 = 100$, $J_2 = 0$.

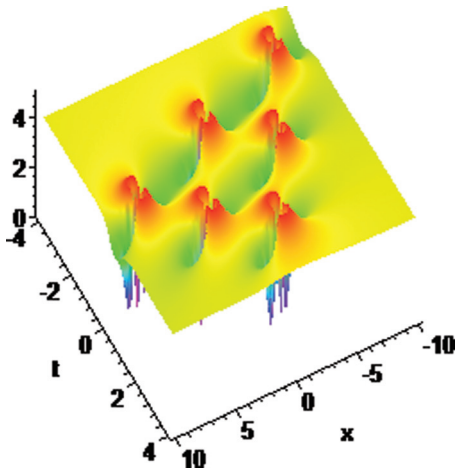

FIG. 20. (Color online) The third-order dark rogue wave $|\tilde{p}^{[3]}|^2$ given by Eq. (26) for the values used in Fig. 19.

waves $\tilde{p}^{[1]}$ and $\tilde{\eta}^{[1]}$, so they are another kind of rogue wave when compared with the typical bright rogue wave $\tilde{E}^{[1]}$, corresponding to the dark breathers in Figs. 2 and 3. So from our earlier understanding of breathers in other physical systems, we call this type of solutions dark rogue waves. Moreover, the dark rogue wave $\tilde{p}^{[1]}$ has one upper ring and three down peaks, and dark rogue wave $\tilde{\eta}^{[1]}$ has two lumps and one down peak. According to analysis, the n-order rogue waves must be generated by an n-order breather solution.

From the detailed literature on rogue waves, to the best of our knowledge, so far only bright rogue waves have been analyzed in detail, but there have been few reports about dark rogue waves in a physical system. In the case of bright optical rogue waves, many results have actually connected the generation of supercontinuum generation (SCG) with rogue waves [63]. In recent years, the supercontinuum white coherent source has attracted a lot of attention because of its potential applications in optical coherence tomography, spectroscopy, wavelength division multiplexing, etc. As reported in Ref. [64], the modulational instability (MI) conditions for the generation of ultrashort pulses have already been investigated in erbium-doped nonlinear fiber, and occurrences of nonconventional side bands have also been observed. This type of nonconventional side band will be very useful to generate a large MI bandwidth, which in turn generates very short pulses. In this way, we believe that our rogue wave results in this paper can also be connected to the generation of SCG. Similarly, the occurrence of dark rogue waves can also be connected to the results of Ref. [64], in the following manner: In our previous work [64], it has been shown that both bright and dark SIT solitons can be generated in the case of the anomalous and normal group velocity dispersion (GVD), in contrast to the well-established results in conventional fiber, where bright and dark solitons exist in the anomalous and normal GVD regions, respectively. From the above results, it is clear that the formation of dark rogue waves can also be connected in a similar way. Thus, it is interesting to analyze the relation connecting the MI, SCG, and rogue wave formation in an optical system.

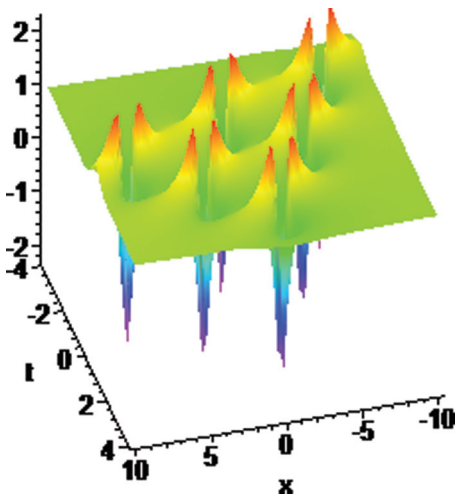

FIG. 21. (Color online) The third-order dark rogue wave $\tilde{\eta}^{[3]}$ given by Eq. (27) for the values used in Fig. 19.

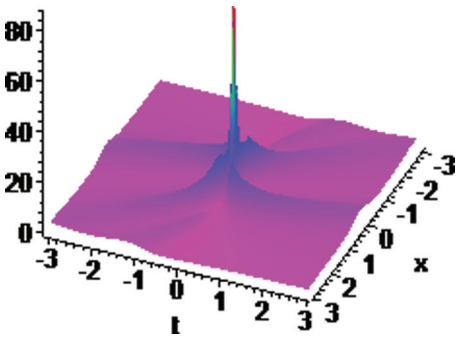

FIG. 22. (Color online) The third-order rogue wave $|\tilde{E}^{[3]}|^2$ given by Eq. (25) with specific parameters $d = \frac{4}{3}$, $b = 0$, $\omega_0 = \frac{1}{2}$, $K_0 = 1$, $J_0 = 0$, $J_1 = 0$, $J_2 = 0$.

IV. CONCLUSION

In this article, we have reported the rogue waves of the three physical fields E, p, and η in a resonant erbium-doped fiber system, which is governed by the NLS-MB equations. These rogue waves are constructed by a Taylor series expansion of the corresponding breather solutions of the NLS-MB equations. As expected, in contrast to the usual bright rogue wave E,

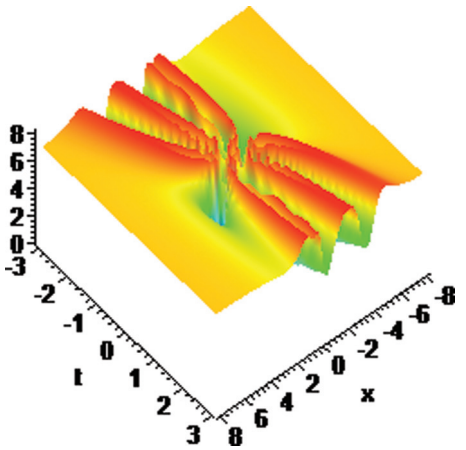

FIG. 23. (Color online) The third-order dark rogue wave $|\tilde{p}^{[3]}|^2$ given by Eq. (26) for the values used in Fig. 22.

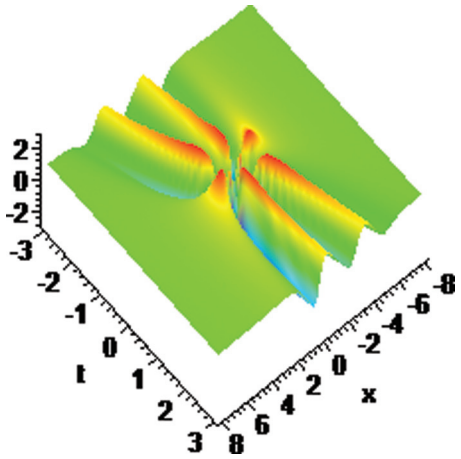

FIG. 24. (Color online) The third-order dark rogue wave $\bar{\eta}^{[3]}$ given by Eq. (27) for the values used in Fig. 22.

we observe dark rogue waves for p and η. The main feature of the dark rogue wave is the appearance of two (or more) dominant down peaks in its profile. In particular, there is one upper ring in the profile of the p, so it may be called the dark-ring rogue wave. The explicit form of $\bar{E}^{[n]}$, $\bar{p}^{[n]}$, and $\bar{\eta}^{[n]}$ is given by the determinant representation of the n-fold DT. The rogue waves in previous section can also be connected to the supercontinuum generation.

As we have already described in the introduction, the singularity [17] of the solutions generated by the DT is the main constraint to generating the dark rogue waves of the defocusing NLS equation. This perhaps shows that the dark rogue wave of the defocusing NLS equation can be investigated by another way, such as by means of Hirota method. From the determinant representation of the T_n, it is interesting to generate the higher-order rogue waves so that the dynamical interactions of rogue waves can be analyzed.

In recent years, considering variable dispersion, variable nonlinearity and variable gain or loss, the investigation of solitons in nonautonomous nonlinear evolution equation equations has also attracted a lot of attention among researchers [65–68]. For example, Serkin and his coworkers have proposed a method to analyze the nonautonomous soliton equations [66–68], and the interaction of solitons in a variable coefficient higher-order NLS equation has been investigated in detail [65]. Using the results of the above papers and making use of our results in this paper, one can also construct the multi-olitons, breathers, and rogue wave solutions of the variable coefficient NLS-MB system. Moreover, it is also possible to obtain a new type of rogue waves for other important coupled system in optics, such as CH-MB equations [69] and variable coefficient CH-MB equations [70,71].

ACKNOWLEDGMENTS

This work is supported by the NSF of China under Grants Nos. 10971109 and 11271210 and the K. C. Wong Magna Fund at Ningbo University. J.H. is also supported by the Natural Science Foundation of Ningbo under Grant No. 2011A610179. K.P. thanks the DST, DAE-BRNS, and UGC, government of India, for financial support through major projects. We thank Prof. Yishen Li (USTC, Hefei, China) for his useful suggestions on the rogue wave.

APPENDIX A

In this appendix, we give expressions for t_1 and elements of T_n:

$$t_1 = \begin{pmatrix} \frac{(\widetilde{Q_n})_{11}}{|W_{2n}|} & \frac{(\widetilde{Q_n})_{12}}{|W_{2n}|} \\ \frac{(\widetilde{Q_n})_{21}}{|W_{2n}|} & \frac{(\widetilde{Q_n})_{22}}{|W_{2n}|} \end{pmatrix},$$

$$W_{2n} = \begin{pmatrix} f_{11} & f_{12} & \lambda_1 f_{11} & \lambda_1 f_{12} & \lambda_1^2 f_{11} & \lambda_1^2 f_{12} & \dots & \lambda_1^{n-1} f_{11} & \lambda_1^{n-1} f_{12} \\ f_{21} & f_{22} & \lambda_2 f_{21} & \lambda_2 f_{22} & \lambda_2^2 f_{21} & \lambda_2^2 f_{22} & \dots & \lambda_2^{n-1} f_{21} & \lambda_2^{n-1} f_{22} \\ f_{31} & f_{32} & \lambda_3 f_{31} & \lambda_3 f_{32} & \lambda_3^2 f_{31} & \lambda_3^2 f_{32} & \dots & \lambda_3^{n-1} f_{31} & \lambda_3^{n-1} f_{32} \\ \vdots & \vdots & \vdots & \vdots & \vdots & \vdots & \vdots & \vdots & \vdots \\ f_{2n1} & f_{2n2} & \lambda_{2n} f_{2n1} & \lambda_{2n} f_{2n2} & \lambda_{2n}^2 f_{2n1} & \lambda_{2n}^2 f_{2n2} & \dots & \lambda_{2n}^{n-1} f_{2n1} & \lambda_{2n}^{n-1} f_{2n2} \end{pmatrix},$$

$$(\widetilde{T_n})_{11} = \begin{vmatrix} 1 & 0 & \lambda & 0 & \lambda^2 & 0 & \dots & \lambda^{n-1} & 0 & \lambda^n \\ f_{11} & f_{12} & \lambda_1 f_{11} & \lambda_1 f_{12} & \lambda_1^2 f_{11} & \lambda_1^2 f_{12} & \dots & \lambda_1^{n-1} f_{11} & \lambda_1^{n-1} f_{12} & \lambda_1^n f_{11} \\ f_{21} & f_{22} & \lambda_2 f_{21} & \lambda_2 f_{22} & \lambda_2^2 f_{21} & \lambda_2^2 f_{22} & \dots & \lambda_2^{n-1} f_{21} & \lambda_2^{n-1} f_{22} & \lambda_2^n f_{21} \\ f_{31} & f_{32} & \lambda_3 f_{31} & \lambda_3 f_{32} & \lambda_3^2 f_{31} & \lambda_3^2 f_{32} & \dots & \lambda_3^{n-1} f_{31} & \lambda_3^{n-1} f_{32} & \lambda_3^n f_{31} \\ \vdots & \vdots & \vdots & \vdots & \vdots & \vdots & \vdots & \vdots & \vdots & \vdots \\ f_{2n1} & f_{2n2} & \lambda_{2n} f_{2n1} & \lambda_{2n} f_{2n2} & \lambda_{2n}^2 f_{2n1} & \lambda_{2n}^2 f_{2n2} & \dots & \lambda_{2n}^{n-1} f_{2n1} & \lambda_{2n}^{n-1} f_{2n2} & \lambda_{2n}^n f_{2n1} \end{vmatrix},$$

$$(\widetilde{T_n})_{12}=\begin{vmatrix} 0 & 1 & 0 & \lambda & 0 & \lambda^2 & \dots & 0 & \lambda^{n-1} & 0\\ f_{11} & f_{12} & \lambda_1 f_{11} & \lambda_1 f_{12} & \lambda_1^2 f_{11} & \lambda_1^2 f_{12} & \dots & \lambda_1^{n-1} f_{11} & \lambda_1^{n-1} f_{12} & \lambda_1^n f_{11}\\ f_{21} & f_{22} & \lambda_2 f_{21} & \lambda_2 f_{22} & \lambda_2^2 f_{21} & \lambda_2^2 f_{22} & \dots & \lambda_2^{n-1} f_{21} & \lambda_2^{n-1} f_{22} & \lambda_2^n f_{21}\\ f_{31} & f_{32} & \lambda_3 f_{31} & \lambda_3 f_{32} & \lambda_3^2 f_{31} & \lambda_3^2 f_{32} & \dots & \lambda_3^{n-1} f_{31} & \lambda_3^{n-1} f_{32} & \lambda_3^n f_{31}\\ \vdots & \vdots & \vdots & \vdots & \vdots & \vdots & \vdots & \vdots & \vdots & \vdots\\ f_{2n1} & f_{2n2} & \lambda_{2n} f_{2n1} & \lambda_{2n} f_{2n2} & \lambda_{2n}^2 f_{2n1} & \lambda_{2n}^2 f_{2n2} & \dots & \lambda_{2n}^{n-1} f_{2n1} & \lambda_{2n}^{n-1} f_{2n2} & \lambda_{2n}^n f_{2n1} \end{vmatrix},$$

$$(\widetilde{T_n})_{21}=\begin{vmatrix} 1 & 0 & \lambda & 0 & \lambda^2 & 0 & \dots & \lambda^{n-1} & 0 & 0\\ f_{11} & f_{12} & \lambda_1 f_{11} & \lambda_1 f_{12} & \lambda_1^2 f_{11} & \lambda_1^2 f_{12} & \dots & \lambda_1^{n-1} f_{11} & \lambda_1^{n-1} f_{12} & \lambda_1^n f_{12}\\ f_{21} & f_{22} & \lambda_2 f_{21} & \lambda_2 f_{22} & \lambda_2^2 f_{21} & \lambda_2^2 f_{22} & \dots & \lambda_2^{n-1} f_{21} & \lambda_2^{n-1} f_{22} & \lambda_2^n f_{22}\\ f_{31} & f_{32} & \lambda_3 f_{31} & \lambda_3 f_{32} & \lambda_3^2 f_{31} & \lambda_3^2 f_{32} & \dots & \lambda_3^{n-1} f_{31} & \lambda_3^{n-1} f_{32} & \lambda_3^n f_{32}\\ \vdots & \vdots & \vdots & \vdots & \vdots & \vdots & \vdots & \vdots & \vdots & \vdots\\ f_{2n1} & f_{2n2} & \lambda_{2n} f_{2n1} & \lambda_{2n} f_{2n2} & \lambda_{2n}^2 f_{2n1} & \lambda_{2n}^2 f_{2n2} & \dots & \lambda_{2n}^{n-1} f_{2n1} & \lambda_{2n}^{n-1} f_{2n2} & \lambda_{2n}^n f_{2n2} \end{vmatrix},$$

$$(\widetilde{T_n})_{22}=\begin{vmatrix} 0 & 1 & 0 & \lambda & 0 & \lambda^2 & \dots & 0 & \lambda^{n-1} & \lambda^n\\ f_{11} & f_{12} & \lambda_1 f_{11} & \lambda_1 f_{12} & \lambda_1^2 f_{11} & \lambda_1^2 f_{12} & \dots & \lambda_1^{n-1} f_{11} & \lambda_1^{n-1} f_{12} & \lambda_1^n f_{12}\\ f_{21} & f_{22} & \lambda_2 f_{21} & \lambda_2 f_{22} & \lambda_2^2 f_{21} & \lambda_2^2 f_{22} & \dots & \lambda_2^{n-1} f_{21} & \lambda_2^{n-1} f_{22} & \lambda_2^n f_{22}\\ f_{31} & f_{32} & \lambda_3 f_{31} & \lambda_3 f_{32} & \lambda_3^2 f_{31} & \lambda_3^2 f_{32} & \dots & \lambda_3^{n-1} f_{31} & \lambda_3^{n-1} f_{32} & \lambda_3^n f_{32}\\ \vdots & \vdots & \vdots & \vdots & \vdots & \vdots & \vdots & \vdots & \vdots & \vdots\\ f_{2n1} & f_{2n2} & \lambda_{2n} f_{2n1} & \lambda_{2n} f_{2n2} & \lambda_{2n}^2 f_{2n1} & \lambda_{2n}^2 f_{2n2} & \dots & \lambda_{2n}^{n-1} f_{2n1} & \lambda_{2n}^{n-1} f_{2n2} & \lambda_{2n}^n f_{2n2} \end{vmatrix},$$

$$(\widetilde{Q_n})_{11}=\begin{vmatrix} f_{11} & f_{12} & \lambda_1 f_{11} & \lambda_1 f_{12} & \lambda_1^2 f_{11} & \lambda_1^2 f_{12} & \dots & \lambda_1^{n-1} f_{12} & \lambda_1^n f_{11}\\ f_{21} & f_{22} & \lambda_2 f_{21} & \lambda_2 f_{22} & \lambda_2^2 f_{21} & \lambda_2^2 f_{22} & \dots & \lambda_2^{n-1} f_{22} & \lambda_2^n f_{21}\\ f_{31} & f_{32} & \lambda_3 f_{31} & \lambda_3 f_{32} & \lambda_3^2 f_{31} & \lambda_3^2 f_{32} & \dots & \lambda_3^{n-1} f_{32} & \lambda_3^n f_{31}\\ \vdots & \vdots & \vdots & \vdots & \vdots & \vdots & \vdots & \vdots & \vdots\\ f_{2n1} & f_{2n2} & \lambda_{2n} f_{2n1} & \lambda_{2n} f_{2n2} & \lambda_{2n}^2 f_{2n1} & \lambda_{2n}^2 f_{2n2} & \dots & \lambda_{2n}^{n-1} f_{2n2} & \lambda_{2n}^n f_{2n1} \end{vmatrix},$$

$$(\widetilde{Q_n})_{12}=-\begin{vmatrix} f_{11} & f_{12} & \lambda_1 f_{11} & \lambda_1 f_{12} & \lambda_1^2 f_{11} & \lambda_1^2 f_{12} & \dots & \lambda_1^{n-1} f_{11} & \lambda_1^n f_{11}\\ f_{21} & f_{22} & \lambda_2 f_{21} & \lambda_2 f_{22} & \lambda_2^2 f_{21} & \lambda_2^2 f_{22} & \dots & \lambda_2^{n-1} f_{21} & \lambda_2^n f_{21}\\ f_{31} & f_{32} & \lambda_3 f_{31} & \lambda_3 f_{32} & \lambda_3^2 f_{31} & \lambda_3^2 f_{32} & \dots & \lambda_3^{n-1} f_{31} & \lambda_3^n f_{31}\\ \vdots & \vdots & \vdots & \vdots & \vdots & \vdots & \vdots & \vdots & \vdots\\ f_{2n1} & f_{2n2} & \lambda_{2n} f_{2n1} & \lambda_{2n} f_{2n2} & \lambda_{2n}^2 f_{2n1} & \lambda_{2n}^2 f_{2n2} & \dots & \lambda_{2n}^{n-1} f_{2n1} & \lambda_{2n}^n f_{2n1} \end{vmatrix},$$

$$(\widetilde{Q_n})_{21}=\begin{vmatrix} f_{11} & f_{12} & \lambda_1 f_{11} & \lambda_1 f_{12} & \lambda_1^2 f_{11} & \lambda_1^2 f_{12} & \dots & \lambda_1^{n-1} f_{12} & \lambda_1^n f_{12}\\ f_{21} & f_{22} & \lambda_2 f_{21} & \lambda_2 f_{22} & \lambda_2^2 f_{21} & \lambda_2^2 f_{22} & \dots & \lambda_2^{n-1} f_{22} & \lambda_2^n f_{22}\\ f_{31} & f_{32} & \lambda_3 f_{31} & \lambda_3 f_{32} & \lambda_3^2 f_{31} & \lambda_3^2 f_{32} & \dots & \lambda_3^{n-1} f_{32} & \lambda_3^n f_{32}\\ \vdots & \vdots & \vdots & \vdots & \vdots & \vdots & \vdots & \vdots & \vdots\\ f_{2n1} & f_{2n2} & \lambda_{2n} f_{2n1} & \lambda_{2n} f_{2n2} & \lambda_{2n}^2 f_{2n1} & \lambda_{2n}^2 f_{2n2} & \dots & \lambda_{2n}^{n-1} f_{2n2} & \lambda_{2n}^n f_{2n2} \end{vmatrix},$$

$$(\widetilde{Q_n})_{22}=-\begin{vmatrix} f_{11} & f_{12} & \lambda_1 f_{11} & \lambda_1 f_{12} & \lambda_1^2 f_{11} & \lambda_1^2 f_{12} & \dots & \lambda_1^{n-1} f_{11} & \lambda_1^n f_{12}\\ f_{21} & f_{22} & \lambda_2 f_{21} & \lambda_2 f_{22} & \lambda_2^2 f_{21} & \lambda_2^2 f_{22} & \dots & \lambda_2^{n-1} f_{21} & \lambda_2^n f_{22}\\ f_{31} & f_{32} & \lambda_3 f_{31} & \lambda_3 f_{32} & \lambda_3^2 f_{31} & \lambda_3^2 f_{32} & \dots & \lambda_3^{n-1} f_{31} & \lambda_3^n f_{32}\\ \vdots & \vdots & \vdots & \vdots & \vdots & \vdots & \vdots & \vdots & \vdots\\ f_{2n1} & f_{2n2} & \lambda_{2n} f_{2n1} & \lambda_{2n} f_{2n2} & \lambda_{2n}^2 f_{2n1} & \lambda_{2n}^2 f_{2n2} & \dots & \lambda_{2n}^{n-1} f_{2n1} & \lambda_{2n}^n f_{2n2} \end{vmatrix}.$$

APPENDIX B

A determinant representation of nth-order DT is constructed in the following form:

$$T_n = T_n(\lambda;\lambda_1,\lambda_2,\dots,\lambda_{2n-1},\lambda_{2n}) = \begin{pmatrix} \frac{(\widehat{T_n})_{11}}{|\widehat{W}_{2n}|} & \frac{(\widehat{T_n})_{12}}{|\widehat{W}_{2n}|} \\ \frac{(\widehat{T_n})_{21}}{|\widehat{W}_{2n}|} & \frac{(\widehat{T_n})_{22}}{|\widehat{W}_{2n}|} \end{pmatrix} \tag{B1}$$

with

$$t_1 = \begin{pmatrix} \frac{(\widehat{Q_n})_{11}}{|\bar{W}_{2n}|} & -\frac{(\widehat{Q_n})_{12}}{|\bar{W}_{2n}|} \\ \frac{(\widehat{Q_n})_{21}}{|\bar{W}_{2n}|} & -\frac{(\widehat{Q_n})_{22}}{|\bar{W}_{2n}|} \end{pmatrix},$$

$$\bar{W}_{2n} = \begin{pmatrix} 1 & \gamma_1 & \lambda_1 & \lambda_1\gamma_1 & \lambda_1^2 & \dots & \lambda_1^{n-1} & \lambda_1^{n-1}\gamma_1 \\ -\gamma_1^* & 1 & \lambda_1^*\gamma_1^* & -\lambda_1^* & -\lambda_1^{*2}\gamma_1^* & \dots & -(-\lambda_1^*)^{n-1}\gamma_1^* & (-\lambda_1^*)^{n-1} \\ 1 & \gamma_3 & \lambda_3 & \lambda_3\gamma_3 & \lambda_3^2 & \dots & \lambda_3^{n-1} & \lambda_3^{n-1}\gamma_3 \\ \vdots & \vdots & \vdots & \vdots & \vdots & \vdots & \vdots & \vdots \\ -\gamma_{2n-1}^* & 1 & \lambda_{2n-1}^*\gamma_{2n-1}^* & -\lambda_{2n-1}^* & -\lambda_{2n-1}^{*2}\gamma_{2n-1}^* & \dots & -(-\lambda_{2n-1}^*)^{n-1}\gamma_{2n-1}^* & (-\lambda_{2n-1}^*)^{n-1} \end{pmatrix},$$

$$(\widehat{T_n})_{11} = \begin{vmatrix} 1 & 0 & \lambda & \dots & \lambda^{n-1} & 0 & \lambda^n \\ 1 & \gamma_1 & \lambda_1 & \dots & \lambda_1^{n-1} & \lambda_1^{n-1}\gamma_1 & \lambda_1^n \\ -\gamma_1^* & 1 & \lambda_1^*\gamma_1^* & \dots & -(-\lambda_1^*)^{n-1}\gamma_1^* & (-\lambda_1^*)^{n-1} & -(-\lambda_1^*)^n\gamma_1^* \\ 1 & \gamma_3 & \lambda_3 & \dots & \lambda_3^{n-1} & \lambda_3^{n-1}\gamma_3 & \lambda_3^n \\ \vdots & \vdots & \vdots & \vdots & \vdots & \vdots & \vdots \\ -\gamma_{2n-1}^* & 1 & \lambda_{2n-1}^*\gamma_{2n-1}^* & \dots & -(-\lambda_{2n-1}^*)^{n-1}\gamma_{2n-1}^* & (-\lambda_{2n-1}^*)^{n-1} & -(-\lambda_{2n-1}^*)^n\gamma_{2n-1}^* \end{vmatrix},$$

$$(\widehat{T_n})_{12} = \begin{vmatrix} 0 & 1 & 0 & \dots & 0 & \lambda^{n-1} & 0 \\ 1 & \gamma_1 & \lambda_1 & \dots & \lambda_1^{n-1} & \lambda_1^{n-1}\gamma_1 & \lambda_1^n \\ -\gamma_1^* & 1 & \lambda_1^*\gamma_1^* & \dots & -(-\lambda_1^*)^{n-1}\gamma_1^* & (-\lambda_1^*)^{n-1} & -(-\lambda_1^*)^n\gamma_1^* \\ 1 & \gamma_3 & \lambda_3 & \dots & \lambda_3^{n-1} & \lambda_3^{n-1}\gamma_3 & \lambda_3^n \\ \vdots & \vdots & \vdots & \vdots & \vdots & \vdots & \vdots \\ -\gamma_{2n-1}^* & 1 & \lambda_{2n-1}^*\gamma_{2n-1}^* & \dots & -(-\lambda_{2n-1}^*)^{n-1}\gamma_{2n-1}^* & (-\lambda_{2n-1}^*)^{n-1} & -(-\lambda_{2n-1}^*)^n\gamma_{2n-1}^* \end{vmatrix},$$

$$(\widehat{T_n})_{21} = \begin{vmatrix} 1 & 0 & \lambda & \dots & \lambda^{n-1} & 0 & 0 \\ 1 & \gamma_1 & \lambda_1 & \dots & \lambda_1^{n-1} & \lambda_1^{n-1}\gamma_1 & \lambda_1^n\gamma_1 \\ -\gamma_1^* & 1 & \lambda_1^*\gamma_1^* & \dots & -(-\lambda_1^*)^{n-1}\gamma_1^* & (-\lambda_1^*)^{n-1} & (-\lambda_1^*)^n \\ 1 & \gamma_3 & \lambda_3 & \dots & \lambda_3^{n-1} & \lambda_3^{n-1}\gamma_3 & \lambda_3^n\gamma_3 \\ \vdots & \vdots & \vdots & \vdots & \vdots & \vdots & \vdots \\ -\gamma_{2n-1}^* & 1 & \lambda_{2n-1}^*\gamma_{2n-1}^* & \dots & -(-\lambda_{2n-1}^*)^{n-1}\gamma_{2n-1}^* & (-\lambda_{2n-1}^*)^{n-1} & (-\lambda_{2n-1}^*)^n \end{vmatrix},$$

$$(\widehat{T_n})_{22} = \begin{vmatrix} 0 & 1 & 0 & \dots & 0 & \lambda^{n-1} & \lambda^n \\ 1 & \gamma_1 & \lambda_1 & \dots & \lambda_1^{n-1} & \lambda_1^{n-1}\gamma_1 & \lambda_1^n\gamma_1 \\ -\gamma_1^* & 1 & \lambda_1^*\gamma_1^* & \dots & -(-\lambda_1^*)^{n-1}\gamma_1^* & (-\lambda_1^*)^{n-1} & (-\lambda_1^*)^n \\ 1 & \gamma_3 & \lambda_3 & \dots & \lambda_3^{n-1} & \lambda_3^{n-1}\gamma_3 & \lambda_3^n\gamma_3 \\ \vdots & \vdots & \vdots & \vdots & \vdots & \vdots & \vdots \\ -\gamma_{2n-1}^* & 1 & \lambda_{2n-1}^*\gamma_{2n-1}^* & \dots & -(-\lambda_{2n-1}^*)^{n-1}\gamma_{2n-1}^* & (-\lambda_{2n-1}^*)^{n-1} & (-\lambda_{2n-1}^*)^n \end{vmatrix},$$

$$(\widehat{Q_n})_{11} = \begin{vmatrix} 1 & \gamma_1 & \lambda_1 & \lambda_1\gamma_1 & \lambda_1^2 & \dots & \lambda_1^{n-1}\gamma_1 & \lambda_1^n \\ -\gamma_1^* & 1 & \lambda_1^*\gamma_1^* & -\lambda_1^* & -\lambda_1^{*2}\gamma_1^* & \dots & (-\lambda_1^*)^{n-1} & -(-\lambda_1^*)^n\gamma_1^* \\ 1 & \gamma_3 & \lambda_3 & \lambda_3\gamma_3 & \lambda_3^2 & \dots & \lambda_3^{n-1}\gamma_3 & \lambda_3^n \\ \vdots & \vdots & \vdots & \vdots & \vdots & \vdots & \vdots & \vdots \\ -\gamma_{2n-1}^* & 1 & \lambda_{2n-1}^*\gamma_{2n-1}^* & -\lambda_{2n-1}^* & -\lambda_{2n-1}^{*2}\gamma_{2n-1}^* & \dots & (-\lambda_{2n-1}^*)^{n-1} & -(-\lambda_{2n-1}^*)^n\gamma_{2n-1}^* \end{vmatrix},$$

$$(\widehat{Q_n})_{12} = \begin{vmatrix} 1 & \gamma_1 & \lambda_1 & \lambda_1\gamma_1 & \dots & \lambda_1^{n-1} & \lambda_1^n \\ -\gamma_1^* & 1 & \lambda_1^*\gamma_1^* & -\lambda_1^* & \dots & -(-\lambda_1^*)^{n-1}\gamma_1^* & -(-\lambda_1^*)^n\gamma_1^* \\ 1 & \gamma_3 & \lambda_3 & \lambda_3\gamma_3 & \dots & \lambda_3^{n-1} & \lambda_3^n \\ \vdots & \vdots & \vdots & \vdots & \vdots & \vdots & \vdots \\ -\gamma_{2n-1}^* & 1 & \lambda_{2n-1}^*\gamma_{2n-1}^* & -\lambda_{2n-1}^* & \dots & -(-\lambda_{2n-1}^*)^{n-1}\gamma_{2n-1}^* & -(-\lambda_{2n-1}^*)^n\gamma_{2n-1}^* \end{vmatrix},$$

$$(\widehat{Q_n})_{21} = \begin{vmatrix} 1 & \gamma_1 & \lambda_1 & \lambda_1\gamma_1 & \lambda_1^2 & \dots & \lambda_1^{n-1}\gamma_1 & \lambda_1^n\gamma_1 \\ -\gamma_1^* & 1 & \lambda_1^*\gamma_1^* & -\lambda_1^* & -\lambda_1^{*2}\gamma_1^* & \dots & (-\lambda_1^*)^{n-1} & (-\lambda_1^*)^n \\ 1 & \gamma_3 & \lambda_3 & \lambda_3\gamma_3 & \lambda_3^2 & \dots & \lambda_3^{n-1}\gamma_3 & \lambda_3^n\gamma_3 \\ \vdots & \vdots & \vdots & \vdots & \vdots & \vdots & \vdots & \vdots \\ -\gamma_{2n-1}^* & 1 & \lambda_{2n-1}^*\gamma_{2n-1}^* & -\lambda_{2n-1}^* & -\lambda_{2n-1}^{*2}\gamma_{2n-1}^* & \dots & (-\lambda_{2n-1}^*)^{n-1} & (-\lambda_{2n-1}^*)^n \end{vmatrix},$$

$$(\widehat{Q_n})_{22} = \begin{vmatrix} 1 & \gamma_1 & \lambda_1 & \lambda_1\gamma_1 & \lambda_1^2 & \dots & \lambda_1^{n-1} & \lambda_1^n\gamma_1 \\ -\gamma_1^* & 1 & \lambda_1^*\gamma_1^* & -\lambda_1^* & -\lambda_1^{*2}\gamma_1^* & \dots & -(-\lambda_1^*)^{n-1}\gamma_1^* & (-\lambda_1^*)^n \\ 1 & \gamma_3 & \lambda_3 & \lambda_3\gamma_3 & \lambda_3^2 & \dots & \lambda_3^{n-1} & \lambda_3^n\gamma_3 \\ \vdots & \vdots & \vdots & \vdots & \vdots & \vdots & \vdots & \vdots \\ -\gamma_{2n-1}^* & 1 & \lambda_{2n-1}^*\gamma_{2n-1}^* & -\lambda_{2n-1}^* & -\lambda_{2n-1}^{*2}\gamma_{2n-1}^* & \dots & -(-\lambda_{2n-1}^*)^{n-1}\gamma_{2n-1}^* & (-\lambda_{2n-1}^*)^n \end{vmatrix}.$$

Here

$$\gamma_{2k-1} = \frac{v_1}{v_2},$$

$$\begin{aligned} v_1 = {} & \left\{ 2i\left(\alpha_{2k-1}^2 - d^2\right) \sin\left[\frac{\sqrt{d^2-\alpha_{2k-1}^2}(-s_2x+s_4t)}{s_2}\right] \cos\left[\frac{\sqrt{d^2-\alpha_{2k-1}^2}(-s_2x+s_4t)}{s_2}\right] \right. \\ & + i\left(-\alpha_{2k-1}^2 + d^2\right) \sin\left[\frac{2\sqrt{d^2-\alpha_{2k-1}^2}(-s_2x+s_4t)}{s2}\right] - 2d\alpha_{2k-1} \cosh\left(\frac{2\sqrt{d^2-\alpha_{2k-1}^2}s_3t}{s_2}\right) \\ & \left. + 2d^2 \cos\left[\frac{2\sqrt{d^2-\alpha_{2k-1}^2}(-s_2x+s_4t)}{s_2}\right] + 2id \sinh\left(\frac{2\sqrt{d^2-\alpha_{2k-1}^2}s_3t}{s_2}\right)\sqrt{d^2-\alpha_{2k-1}^2} \right\} \exp(-is_1), \\ v_2 = {} & \left(-2d^2 + 2\alpha_{2k-1}^2\right) \sinh\left(\frac{\sqrt{d^2-\alpha_{2k-1}^2}s_3t}{s_2}\right) \cosh\left(\frac{\sqrt{d^2-\alpha_{2k-1}^2}s_3t}{s_2}\right) + 2d^2 \cosh\left(\frac{2\sqrt{d^2-\alpha_{2k-1}^2}s_3t}{s_2}\right) \\ & + \left(d^2 - \alpha_{2k-1}^2\right) \sinh\left(\frac{2\sqrt{d^2-\alpha_{2k-1}^2}s_3t}{s_2}\right) - 2\sqrt{d^2-\alpha_{2k-1}^2}d \sin\left[\frac{2\sqrt{d^2-\alpha_{2k-1}^2}(-s_2x+s_4t)}{s_2}\right] \\ & - 2d\alpha_{2k-1} \cos\left[2\frac{\sqrt{d^2-\alpha_{2k-1}^2}(-s_2x+s_4t)}{s_2}\right], \end{aligned} \tag{B2}$$

$$s_1 = \frac{-b(1/2b-\omega_0)x + [2 + 2(1/2b-\omega_0)(1/4b^2 - 1/2d^2)]t}{-1/2b+\omega_0},$$

$$s_2 = (-1/2b+\omega_0)[(1/2b-\omega_0)^2 + d^2],$$

$$s_3 = -d\omega_0(d^2+\omega_0^2) - 3/2db\omega_0(1/2b-\omega_0) + 1/2db(d^2+1/4b^2) + d,$$

$$s_4 = -1/2b^2(d^2+1/4b^2) + b\omega_0(d^2+\omega_0{}^2) + 3/2b^2\omega_0(1/2b-\omega_0) + 1/2b - \omega_0.$$

APPENDIX C

Here we give the construction of T of $\bar{T}_{rn}(\lambda)$ in detail:

$$\bar{T}_{rn} = \bar{T}_{rn}(\lambda) = \begin{pmatrix} \frac{(\widetilde{T_{rn}})_{11}}{|W_{r2n}|} & \frac{(\widetilde{T_{rn}})_{12}}{|W_{r2n}|} \\ \frac{(\widetilde{T_{rn}})_{21}}{|W_{r2n}|} & \frac{(\widetilde{T_{rn}})_{22}}{|W_{r2n}|} \end{pmatrix}, \tag{C1}$$

$$\bar{t}_{r1} = \begin{pmatrix} \frac{(\widetilde{Q_{rn}})_{11}}{|W_{r2n}|} & \frac{(\widetilde{Q_{rn}})_{12}}{|W_{r2n}|} \\ \frac{(\widetilde{Q_{rn}})_{21}}{|W_{r2n}|} & \frac{(\widetilde{Q_{rn}})_{22}}{|W_{r2n}|} \end{pmatrix},$$

$$W_{r2n}=\begin{pmatrix} h_{01}^{1} & h_{02}^{1} & h_{11}^{1} & h_{12}^{1} & \cdots & h_{n-11}^{1} & h_{n-12}^{1} \\ -h_{02}^{1*} & h_{01}^{1*} & h_{12}^{1*} & -h_{11}^{1*} & \cdots & (-1)^{n}h_{n-12}^{1*} & (-1)^{n-1}h_{n-11}^{1*} \\ h_{01}^{3} & h_{02}^{3} & h_{11}^{3} & h_{12}^{3} & \cdots & h_{n-11}^{3} & h_{n-12}^{3} \\ \vdots & \vdots & \vdots & \vdots & \vdots & \vdots & \vdots \\ -h_{02}^{2n-1*} & h_{01}^{2n-1*} & h_{12}^{2n-1*} & -h_{11}^{2n-1*} & \cdots & (-1)^{n}h_{n-12}^{2n-1*} & (-1)^{n-1}h_{n-11}^{2n-1^{*}} \end{pmatrix},$$

$$(\widetilde{T_{rn}})_{11}=\begin{vmatrix} 1 & 0 & \lambda & 0 & \cdots & \lambda^{n-1} & 0 & \lambda^{n} \\ h_{01}^{1} & h_{02}^{1} & h_{11}^{1} & h_{12}^{1} & \cdots & h_{n-11}^{1} & h_{n-12}^{1} & h_{n1}^{1} \\ -h_{02}^{1*} & h_{01}^{1*} & h_{12}^{1*} & -h_{11}^{1*} & \cdots & (-1)^{n}h_{n-12}^{1*} & (-1)^{n-1}h_{n-11}^{1*} & (-1)^{n+1}{h_{n2}}^{1*} \\ h_{01}^{3} & h_{02}^{3} & h_{11}^{3} & h_{12}^{3} & \cdots & h_{n-11}^{3} & h_{n-12}^{3} & h_{n1}^{3} \\ \vdots & \vdots & \vdots & \vdots & \vdots & \vdots & \vdots & \vdots \\ -h_{02}^{2n-1*} & h_{01}^{2n-1*} & h_{12}^{2n-1*} & -h_{11}^{2n-1*} & \cdots & (-1)^{n}h_{n-12}^{2n-1*} & (-1)^{n-1}h_{n-11}^{2n-1*} & (-1)^{n+1}{h_{n2}}^{2n-1*} \end{vmatrix},$$

$$(\widetilde{T_{rn}})_{12}=\begin{vmatrix} 0 & 1 & 0 & \lambda & \cdots & 0 & \lambda^{n-1} & 0 \\ h_{01}^{1} & h_{02}^{1} & h_{11}^{1} & h_{12}^{1} & \cdots & h_{n-11}^{1} & h_{n-12}^{1} & h_{n1}^{1} \\ -h_{02}^{1*} & h_{01}^{1*} & h_{12}^{1*} & -h_{11}^{1*} & \cdots & (-1)^{n}h_{n-12}^{1*} & (-1)^{n-1}h_{n-11}^{1*} & (-1)^{n+1}{h_{n2}}^{1*} \\ h_{01}^{3} & h_{02}^{3} & h_{11}^{3} & h_{12}^{3} & \cdots & h_{n-11}^{3} & h_{n-12}^{3} & h_{n1}^{3} \\ \vdots & \vdots & \vdots & \vdots & \vdots & \vdots & \vdots & \vdots \\ -h_{02}^{2n-1*} & h_{01}^{2n-1*} & h_{12}^{2n-1*} & -h_{11}^{2n-1*} & \cdots & (-1)^{n}h_{n-12}^{2n-1*} & (-1)^{n-1}h_{n-11}^{2n-1*} & (-1)^{n+1}{h_{n2}}^{2n-1*} \end{vmatrix},$$

$$(\widetilde{T_{rn}})_{21}=\begin{vmatrix} 1 & 0 & \lambda & 0 & \cdots & \lambda^{n-1} & 0 & 0 \\ h_{01}^{1} & h_{02}^{1} & h_{11}^{1} & h_{12}^{1} & \cdots & h_{n-11}^{1} & h_{n-12}^{1} & h_{n2}^{1} \\ -h_{02}^{1*} & h_{01}^{1*} & h_{12}^{1*} & -h_{11}^{1*} & \cdots & (-1)^{n}h_{n-12}^{1*} & (-1)^{n-1}h_{n-11}^{1*} & (-1)^{n}h_{n1}^{1*} \\ h_{01}^{3} & h_{02}^{3} & h_{11}^{3} & h_{12}^{3} & \cdots & h_{n-11}^{3} & h_{n-12}^{3} & h_{n2}^{3} \\ \vdots & \vdots & \vdots & \vdots & \vdots & \vdots & \vdots & \vdots \\ -h_{02}^{2n-1*} & h_{01}^{2n-1*} & h_{12}^{2n-1*} & -h_{11}^{2n-1*} & \cdots & (-1)^{n}h_{n-12}^{2n-1*} & (-1)^{n-1}h_{n-11}^{2n-1*} & (-1)^{n}h_{n1}^{2n-1*} \end{vmatrix},$$

$$(\widetilde{T_{rn}})_{22}=\begin{vmatrix} 0 & 1 & 0 & \lambda & \cdots & 0 & \lambda^{n-1} & \lambda^{n} \\ h_{01}^{1} & h_{02}^{1} & h_{11}^{1} & h_{12}^{1} & \cdots & h_{n-11}^{1} & h_{n-12}^{1} & h_{n2}^{1} \\ -h_{02}^{1*} & h_{01}^{1*} & h_{12}^{1*} & -h_{11}^{1*} & \cdots & (-1)^{n}h_{n-12}^{1*} & (-1)^{n-1}h_{n-11}^{1*} & (-1)^{n}h_{n1}^{1*} \\ h_{01}^{3} & h_{02}^{3} & h_{11}^{3} & h_{12}^{3} & \cdots & h_{n-11}^{3} & h_{n-12}^{3} & h_{n2}^{3} \\ \vdots & \vdots & \vdots & \vdots & \vdots & \vdots & \vdots & \vdots \\ -h_{02}^{2n-1*} & h_{01}^{2n-1*} & h_{12}^{2n-1*} & -h_{11}^{2n-1*} & \cdots & (-1)^{n}h_{n-12}^{2n-1*} & (-1)^{n-1}h_{n-11}^{2n-1*} & (-1)^{n}h_{n1}^{2n-1*} \end{vmatrix},$$

$$(\widetilde{Q_{rn}})_{11}=\begin{vmatrix} h_{01}^{1} & h_{02}^{1} & h_{11}^{1} & h_{12}^{1} & \cdots & h_{n-12}^{1} & h_{n1}^{1} \\ -h_{02}^{1*} & h_{01}^{1*} & h_{12}^{1*} & -h_{11}^{1*} & \cdots & (-1)^{n-1}h_{n-11}^{1*} & (-1)^{n+1}{h_{n2}}^{1*} \\ h_{01}^{3} & h_{02}^{3} & h_{11}^{3} & h_{12}^{3} & \cdots & h_{n-12}^{3} & h_{n1}^{3} \\ \vdots & \vdots & \vdots & \vdots & \vdots & \vdots & \vdots \\ -h_{02}^{2n-1*} & h_{01}^{2n-1*} & h_{12}^{2n-1*} & -h_{11}^{2n-1*} & \cdots & (-1)^{n-1}h_{n-11}^{2n-1*} & (-1)^{n+1}{h_{n2}}^{2n-1*} \end{vmatrix},$$

$$(\widetilde{Q_{rn}})_{12}=-\begin{vmatrix} h_{01}^{1} & h_{02}^{1} & h_{11}^{1} & h_{12}^{1} & \cdots & h_{n-11}^{1} & h_{n1}^{1} \\ -h_{02}^{1*} & h_{01}^{1*} & h_{12}^{1*} & -h_{11}^{1*} & \cdots & (-1)^{n}h_{n-12}^{1*} & (-1)^{n+1}{h_{n2}}^{1*} \\ h_{01}^{3} & h_{02}^{3} & h_{11}^{3} & h_{12}^{3} & \cdots & h_{n-11}^{3} & h_{n1}^{3} \\ \vdots & \vdots & \vdots & \vdots & \vdots & \vdots & \vdots \\ -h_{02}^{2n-1*} & h_{01}^{2n-1*} & h_{12}^{2n-1*} & -h_{11}^{2n-1*} & \cdots & (-1)^{n}h_{n-12}^{2n-1*} & (-1)^{n+1}{h_{n2}}^{2n-1*} \end{vmatrix},$$

$$(\widetilde{Q_{rn}})_{21}=\begin{vmatrix} h_{01}^{1} & h_{02}^{1} & h_{11}^{1} & h_{12}^{1} & \cdots & h_{n-12}^{1} & h_{n2}^{1} \\ -h_{02}^{1*} & h_{01}^{1*} & h_{12}^{1*} & -h_{11}^{1*} & \cdots & (-1)^{n-1}h_{n-11}^{1*} & (-1)^{n}h_{n1}^{1*} \\ h_{01}^{3} & h_{02}^{3} & h_{11}^{3} & h_{12}^{3} & \cdots & h_{n-12}^{3} & h_{n2}^{3} \\ \vdots & \vdots & \vdots & \vdots & \vdots & \vdots & \vdots \\ -h_{02}^{2n-1*} & h_{01}^{2n-1*} & h_{12}^{2n-1*} & -h_{11}^{2n-1*} & \cdots & (-1)^{n-1}h_{n-11}^{2n-1*} & (-1)^{n}h_{n1}^{2n-1*} \end{vmatrix},$$

$$(\widetilde{Q_{rn}})_{22} = -\begin{vmatrix} h_{01}^{1} & h_{02}^{1} & h_{11}^{1} & h_{12}^{1} & \cdots & h_{n-11}^{1} & h_{n2}^{1} \\ -h_{02}^{1*} & h_{01}^{1*} & h_{12}^{1*} & -h_{11}^{1*} & \cdots & (-1)^n h_{n-12}^{1*} & (-1)^n h_{n1}^{1*} \\ h_{01}^{3} & h_{02}^{3} & h_{11}^{3} & h_{12}^{3} & \cdots & h_{n-11}^{3} & h_{n2}^{3} \\ \vdots & \vdots & \vdots & \vdots & \vdots & \vdots & \vdots \\ -h_{02}^{2n-1*} & h_{01}^{2n-1*} & h_{12}^{2n-1*} & -h_{11}^{2n-1*} & \cdots & (-1)^n h_{n-12}^{2n-1*} & (-1)^n h_{n1}^{2n-1*} \end{vmatrix}.$$

Here

$$h_{mj}^{l} = \frac{\partial^l}{\partial \delta^l}\left[\left(d + i\frac{b}{2} + \delta^2\right)^m f_{1j}\left(\lambda_1 = d + i\frac{b}{2} + \delta^2\right)\right]\Big|_{\delta=0}, \quad m = 0,1,2,\ldots n, j = 1,2, l = 1,2,\ldots 2n.$$

[1] A. Hasegawa and F. Tappert, Appl. Phys. Lett. **23**, 142 (1973).
[2] S. L. McCall and E. L. Hahn, Phys. Rev. Lett. **18**, 908 (1967).
[3] A. I. Maimistov and E. A. Manykin, Sov. Phys. JETP **58**, 685 (1983).
[4] A. I. Maimistov and E. A. Manykin, Sov. Phys. JETP. **85**, 1177 (1983).
[5] A. I. Maimistov and A. M. Basharov, *Nonlinear Optical Waves* (Springer-Verlag, Berlin, 1999).
[6] K. Porsezian and K. Nakkeeran, J. Mod. Opt. **42**, 1953 (1995).
[7] S. Kakei and J. Satsuma, J. Phys. Soc. Jpn. **63**, 885 (1994).
[8] M. Nakazawa, E. Yamada, and H. Kubota, Phys. Rev. Lett. **66**, 2625 (1991).
[9] M. Nakazawa, E. Yamada, and H. Kubota, Phys. Rev. A **44**, 5973 (1991).
[10] M. Nakazawa, Y. Kimura, K. Kurokawa, and K. Suzuki, Phys. Rev. A **45**, R23 (1992).
[11] M. Nakazawa, K. Suzuki, Y. Kimura, and H. Kubota, Phys. Rev. A **45**, R2682 (1992).
[12] K. Porsezian and K. Nakkeeran, Phys. Rev. Lett. **74**, 2941 (1995).
[13] K. Porsezian, P. Seenuvasakumaran, and R. Ganapathy, Phys. Lett. A **348**, 233 (2006).
[14] A. Mahalingam, K. Porsezian, M. S. Mani Rajan, and A. Uthayakumar, J. Phys. A: Math. Theor. **42**, 165101 (2009).
[15] C. G. Latchio Tiofack, A. Mohamadou, T. C. Kofane, and K. Porsezian, J. Opt. **12**, 085202 (2010).
[16] J. S. He, Y. Cheng, and Y. S. Li, Commun. Theor. Phys. **38**, 493 (2002).
[17] G. Neugebauer and R. Meinel, Phys. Lett. A **100**, 467 (1984).
[18] V. B. Matveev and M. A. Salle, *Darboux Transfromations and Solitons* (Springer-Verlag, Berlin, 1991).
[19] G. Rui, T. Bo, L. Xing, Z. Hai-Qiang, and L. Wen-Jun, Comput. Math. Math. Phys. **52**, 565 (2012).
[20] Ming Wang, Wen-Rui Shan, Xing Lü, Bo Qin, and Li-Cai Liu, Z. Naturforsch. A **66**, 712 (2011).
[21] C. Kharif and E. Pelinovsky, Eur. J. Mech. B (Fluids). **22**, 603 (2003).
[22] C. Kharif, E. Pelinovsky, and A. Slunyaev, *Rogue Waves in the Ocean* (Springer, Berlin, 2009).
[23] A. Chabchoub, N. P. Hoffmann, and N. Akhmediev, Phys. Rev. Lett. **106**, 204502 (2011).
[24] I. Didenkulova1 and E. Pelinovsky, Nonlinearity **24**, R1 (2011).
[25] D. H. Peregrine, J. Aust. Math. Soc. Series B, Appl. Math. **25**, 16 (1983).
[26] K. B. Dysthe and K. Trulsen, Phys. Scr. **82**, 48 (1999).
[27] V. E. Zakharov and L. A. Ostrovsky, Phys. D **238**, 540 (2009).
[28] N. N. Akhmediev and V. I. Korneev, Theor. Math. Phys. **69**, 1080 (1986).
[29] I. Shrira and V. Geogjaev, J. Eng. Math. **67**, 11 (2010).
[30] Z. Yan, Phys. Lett. A **374**, 672 (2009).
[31] C. Q. Dai, G. Q. Zhou, and J. F. Zhang, Phys. Rev. E **85**, 016603 (2012).
[32] L. H. Ying, Z. Zhuang, E. J. Heller, and L. Kaplan, Nonlinearity **24**, R67 (2011).
[33] P. Dubard, P. Gaillard, C. Klein, and V. B. Matveev, Eur. Phys. J. Special Topics **185**, 247 (2010).
[34] P. Dubard and V. B. Matveev, Nat. Hazards Earth Syst. Sci. **11**, 667 (2011).
[35] P. Gaillard, J. Phys. A: Math. Theor. **44**, 435204 (2011).
[36] G. Boling, L. Ling, and Q. P. Liu, Phys. Rev. E **85**, 026607 (2012).
[37] Y. Ohta and J. Yang, Proc. R. Soc. A **468**, 1716 (2012).
[38] N. Akhmediev, J. M. Soto-Crespo, and A. Ankiewicz, Phys. Rev. A. **80**, 043818 (2009).
[39] J. S. He, H. R. Zhang, L. H. Wang, K. Porsezian, and A. S. Fokas, arXiv:1209.3742v3 (2012).
[40] V. Fedun, M. S. Ruderman, and R. Erdélyi, Phys. Lett. A **372**, 6107 (2008).
[41] M. S. Ruderman, Eur. Phys. J. **185**, 57 (2010).
[42] S. Xu, J. He, and L. Wang, J. Phys. A: Math. Theor. **44**, 305203 (2011).
[43] S. Xu, J. He, and L. Wang, Europhys. Lett. **97**, 30007 (2012).
[44] W. M. Moslem, P. K. Shukla, and B. Eliasson, Europhys. Lett. **96**, 25002 (2011).
[45] B. Guo, L. Ling, and Q. P. Liu, Stud. Appl. Math. (2012), doi: 10.1111/j.1467-9590.2012.00568.x.
[46] D. R. Solli, C. Ropers, P. Koonath, and B. Jalali, Nature (London) **450**, 1054 (2007).

[47] B. Kibler, J. Fatome, C. Finot, G. Millot, F. Dias, G. Genty, N. Akhmediev, and J. M. Dudley, Nature Phys. **6**, 790 (2010).
[48] F. T. Arecchi, U. Bortolozzo, A. Montina, and S. Residori, Phys. Rev. Lett. **106**, 153901 (2011).
[49] A. Ankiewicz, J. M. Soto-Crespo, and N. Akhmediev, Phys. Rev. E **81**, 046602 (2010).
[50] G. Yang, L. Li, and S. Jia, Phys. Rev. E **85**, 046608 (2012).
[51] Y. Tao and J. He, Phys. Rev. E **85**, 026601 (2012).
[52] A. Ankiewicz, N. Akhmediev, and J. M. Soto-Crespo, Phys. Rev. E **82**, 026602 (2010).
[53] G. Boling and L. Ling, Chin. Phys. Lett. **28**, 110202 (2011).
[54] F. Baronio, A. Degasperis, M. Conforti, and S. Wabnitz, Phys. Rev. Lett. **109**, 044102 (2012).
[55] B.-G. Zhai, W.-G. Zhang, X.-L. Wang, and H.-Q. Zhang, Nonlinear Anal. RWA **14**, 14 (2012).
[56] Z. Qin and G. Mu, Phys. Rev. E **86**, 036601 (2012).
[57] R. Jaimes-Reátegui, R. Sevilla-Escoboza, and G. Huerta-Cuellar, Phys. Rev. Lett. **107**, 274101 (2011).
[58] V. E. Zakharov and A. B. Shabat, Sov. Phys. JETP **37**, 823 (1973).
[59] J. He, S. Xu, and K. Porsezian, J. Phys. Soc. Jpn. **81**, 033002 (2012).
[60] J. S. He, L. Zhang, Y. Cheng, and Y. S. Li, Sci. China A: Math. **12**, 1867 (2006).
[61] A. Ankiewicz, J. D. Kedziora, and N. Akhmediev, Phys. Lett. A **375**, 2782 (2011).
[62] D. J. Kedziora, A. Ankiewicz, and N. Akhmediev, Phys. Rev. E **84**, 056611 (2011).
[63] J. M. Dudley and J. R. Taylor, eds., *Supercontinuum Generation in Optical Fibres* (Cambridge University Press, Cambridge, 2010).
[64] B. Kalithasan, K. Porsezian, P. T. Dinda, and B. A. Malomed, J. Opt. A: Pure Appl. Opt. **11**, 045205 (2009).
[65] K. Porsezian, A. Hasegawa, V. N. Serkin, T. L. Belyaeva, and R. Ganapathy, Phys. Lett. A **361**, 504 (2007).
[66] V. N. Serkin and A. Hasegawa, Phys. Rev. Lett. **85**, 4502 (2000).
[67] V. N. Serkin, A. Hasegawa, and T. L. Belyaeva, Phys. Rev. Lett. **98**, 074102 (2007).
[68] V. N. Serkin, A. Hasegawa, and T. L. Belyaeva, J. Mod. Opt. **57**, 1456 (2010).
[69] C. Li, J. He, and K. Porsezian, arXiv:1205.1191v1 (2012).
[70] C. Li and J. He, arXiv:1210.2501 (2012).
[71] Y.-S. Xue, B. Tian, W.-B. Ai, M. Li, and P. Wang, Opt. Laser Technol. **48**, 153 (2013).